

ICRR-Report-643-2012-32

IPMU13-0009

UT-13-01

Axions : Theory and Cosmological Role

Masahiro Kawasaki^(a,b) and Kazunori Nakayama^(c,b)

^a*Institute for Cosmic Ray Research, University of Tokyo, Kashiwa 277-8582, Japan*

^b*Institute for the Physics and Mathematics of the universe, University of Tokyo,
Kashiwa 277-8568, Japan*

^c*Department of Physics, University of Tokyo, Tokyo 113-0033, Japan*

Abstract

We review recent developments on axion cosmology. Topics include : axion cold dark matter, axions from topological defects, axion isocurvature perturbation and its non-Gaussianity and axino/saxion cosmology in supersymmetric axion model.

Contents

1	Introduction	2
2	Peccei-Quinn mechanism and axion	4
2.1	Models of invisible axion	4
2.2	Astrophysical and experimental constraints	5
3	Axion cosmology	7
3.1	Evolution of PQ scalar	7
3.2	Abundance of the axion	9
3.2.1	Cold axion	9
3.2.2	Hot axion	10
3.3	PQ symmetry breaking after inflation	11
3.3.1	Axionic strings	12
3.3.2	Axionic domain walls with $N_{\text{DW}} = 1$	14
3.3.3	Axionic domain walls with $N_{\text{DW}} \geq 2$	16
3.4	PQ symmetry breaking before/during inflation	19
4	Supersymmetry and axion	24
4.1	Stabilization of the PQ scalar	25
4.1.1	Model A	25
4.1.2	Model B	26
4.1.3	Model C	27
4.2	Axino cosmology	28
4.3	Saxion cosmology	30
5	Discussion	33

1 Introduction

The standard model (SM) in particle physics is well established after the discovery of the Higgs-boson like particle at LHC [1, 2]. While it goes without saying that SM is a

successful theory, it suffers from the strong CP problem [3, 4]. The following term in the Lagrangian allowed by the gauge symmetry,

$$\mathcal{L} = \theta \frac{g_s^2}{32\pi^2} G_{\mu\nu}^a \tilde{G}^{\mu\nu a}, \quad (1)$$

violates CP and contributes to the neutron electric dipole moment (NEDM). Here g_s is the QCD gauge coupling constant, $G_{\mu\nu}^a$ is the gluon field strength, $\tilde{G}_{\mu\nu}^a$ is its dual, and θ is a constant parameter. Recent experimental bound on the NEDM reads $|d_n| < 2.9 \times 10^{-26} e \text{ cm}$ (90% CL) [5]. This leads to the constraint on the θ parameter as $\theta < 0.7 \times 10^{-11}$ [3, 4]. There seems to be no reason in the SM why θ must be so small : this is the strong CP problem.

Peccei and Quinn [6, 7] proposed a beautiful solution to the strong CP problem. They introduced anomalous global U(1) symmetry, which we denote by U(1)_{PQ} called PQ symmetry, which is spontaneously broken. Then the θ term is replaced by a dynamical field, which automatically goes to zero by minimizing the potential. It was soon realized that such a solution to the strong CP problem leads to a light pseudo scalar particle : axion [8, 9]. The axion is a pseudo-Nambu Goldstone boson in association with spontaneous breakdown of the PQ symmetry. It has a coupling as

$$\mathcal{L} = \frac{g_s^2}{32\pi^2} \frac{a}{F_a} G_{\mu\nu}^a \tilde{G}^{\mu\nu a}, \quad (2)$$

where a denotes the axion field and F_a is the scale of PQ symmetry breaking. Then the θ parameter is effectively replaced with $\theta + a/F_a$. It has a CP-conserving potential minimum at $\theta + a/F_a = 0$, hence the CP angle is dynamically tuned to be zero without fine-tuning. It is a very attractive idea for solving the strong CP problem.

Once we believe the PQ solution to the strong CP problem, the axion may play an important role in particle phenomenology and cosmology. In this article we review the axion cosmology, in particular focusing on recent developments in the last few years. We do not aim to explain underlying physics of the axion, for which we refer to excellent reviews [3, 4]. In Section 2, the PQ and axion models, and experimental/observational constraints are briefly summarized. In Section 3, we discuss the axion cosmology. In particular, recent calculations on the cold and hot axion abundances, axions emitted from topological defects, and axion isocurvature fluctuation and its non-Gaussianity are

summarized. In Section 4, we focus on supersymmetric (SUSY) axion models and their cosmological effects. There are some recent developments on the evaluation of the saxion and axino abundances. In Section 5, we mention some related topics which are not covered in the main text.

2 Peccei-Quinn mechanism and axion

2.1 Models of invisible axion

Early models of axion [8, 9], where the axion was associated with the weak scale Higgs boson, were soon ruled out experimentally. Currently the most axion models make the axion invisible by assuming very high PQ scale. There are two known class of invisible axion models : KSVZ model (or also called hadronic axion model) [10, 11] and DFSZ model [12, 13].

In the KSVZ model [10, 11], heavy quark pair, Q and \bar{Q} are introduced which are fundamental and anti-fundamental representations of $SU(3)_c$ and couple to the PQ scalar ϕ as

$$\mathcal{L} = k\phi Q\bar{Q}. \quad (3)$$

Here $U(1)_{PQ}$ charges are assigned as $\phi(+1)$, $Q(-1/2)$ and $\bar{Q}(-1/2)$. These quarks become heavy after ϕ gets a vacuum expectation value (VEV) of η , which is related to the PQ scale F_a defined in (2), through the relation $F_a = \eta/N_{DW}$. Here a model-dependent integer N_{DW} is called the domain wall number (See Section 3). All the SM fields are assumed to be singlets under $U(1)_{PQ}$. Clearly, this global $U(1)_{PQ}$ has an anomaly under the QCD. Therefore, the axion obtains a coupling as Equation 2 and the theta angle is dynamically tuned to be zero by the PQ mechanism. For a minimal case where only one pair of heavy quarks is introduced, we have $N_{DW} = 1$. There is no domain wall problem in this case. (See Section 3).

In the DFSZ model [12, 13], the PQ field couples to the SM Higgs. In this model two Higgs doublets are required : H_1 and H_2 . We assume that H_1 transforms as the SM Higgs and H_2 as its conjugation under the SM gauge groups. Moreover, PQ charges are assigned so that the combination $H_1 H_2$ has -1 . Then we can write down the interaction

term among them in the potential of PQ and Higgs sector,

$$-\mathcal{L} = |\phi|^2(c_1|H_1|^2 + c_2|H_2|^2) + c_3|H_1|^2|H_2|^2 + c_4|H_1H_2|^2 + (\mu\phi H_1H_2 + \text{h.c.}), \quad (4)$$

where c_1, \dots, c_4 are numerical constants and μ is a dimensional parameter. Let us suppose that the VEVs of H_1 and H_2 give up- and down-type quark masses. Then up-type SM quarks necessarily have PQ charge and the $U(1)_{\text{PQ}}$ becomes anomalous under the QCD. Hence the axion coupling like Equation 2 appears, solving the strong CP problem. In this case, the domain wall number is calculated as $N_{\text{DW}} = 3$ reflecting three family of SM quarks.¹ Hence it may suffer from the domain wall problem if the PQ symmetry is broken after inflation. A distinct feature of the DFSZ model is that SM fermions, including leptons, have tree-level coupling to the axion through the Higgs-axion mixing.

In the so-called variant axion model [14, 15], it is assumed that H_1 only couples to one family of up-type quarks (say, top quark). All other quarks have zero PQ charges and obtain masses from H_2 . In this case, we have $N_{\text{DW}} = 1$ and there is no domain wall problem. See [16] for implications of Higgs sector in this model at collider experiments.

2.2 Astrophysical and experimental constraints

Since the axion interaction is very weak and much lighter than typical temperature of stars, axions are emitted from stars. Hence the PQ scale is bounded below so as not to change evolutions of stars significantly [17, 18]. The most stringent constraint comes from the observation of SN1987A. In order for the axion emission not to shorten the burst duration, the PQ scale is bounded as $F_a \gtrsim 4 \times 10^8 \text{ GeV}$. This bound relies on the axion-hadron interaction, which always exists in the axion model solving the strong CP problem.² The observation of horizontal branch (HB) stars in globular clusters also set lower bound on the PQ scale as $F_a \gtrsim 10^7 \text{ GeV}$.³

There are activities on experimental searches for the axion.

¹ This depends on PQ charge assignments on the Higgs field. For example, if we take the PQ charge of H_1H_2 to be -2 , the allowed term is $\phi^2 H_1H_2$ and we obtain $N_{\text{DW}} = 6$.

² For much smaller F_a the axion becomes optically thick and the axion emission rate is suppressed. The bound from the burst duration of SN1987A disappears at $F_a \lesssim 10^6 \text{ GeV}$. On the other hand, for even smaller F_a , the detection rate of the thermally emitted axion from SN1987A at the Kamiokande would become large. As a result, the SN1987A does not pose a constraint for $10^5 \text{ GeV} \lesssim F_a \lesssim 10^6 \text{ GeV}$.

³ The bound from HB stars come from axion-photon interaction, which is model-dependent. If the coefficient of the axion-photon-photon interaction is somehow chosen to be much smaller than unity, the

Axion helioscope Axion helioscopes try to detect axions with energy of order keV emitted from the center of the Sun through the axion-photon conversion process under the magnetic field [21]. Currently the CAST experiment [22, 23] put the most stringent bound on the strength of axion-photon-photon coupling in this way. In particular, the resonant conversion expected from the plasma frequency of photon induced by the buffer gas can improve the sensitivity and they begin to cover the parameter region predicted in the QCD axion for $F_a \sim 10^{7-8}$ GeV. The Tokyo axion helioscope also reaches the QCD axion prediction for small range of the axion mass [24]. Future project, called IAXO [25], may reveal the QCD axion for $F_a \sim 10^9$ GeV.

Axion haloscope Axion haloscopes try to detect dark matter (DM) axions in the Galaxy by using the microwave cavity [21, 26]. Under the magnetic field, the axion DM may produce radio wave with its frequency corresponding to the axion mass, and it is amplified if the size of the cavity matches with the Compton wave length of the axion. Note that this technique crucially relies on the assumption that the observed DM consists of cold axion. The ADMX experiment already begins to exclude axion DM for a limited range of the axion mass around $F_a \sim 10^{11}$ GeV [27]. It is expected to cover the wide range of parameters consistent with axion DM.

Laser searches Axion mixes with the photon in the external magnetic field due to the axion-photon-photon interaction term. The “light shining through a wall” experiments utilize the laser, a part of whose light would pass through a wall as axions under the magnetic field. The ALPS collaboration placed the most strict bound by this idea [28], although currently it does not reach the CAST sensitivity and the bound from HB star cooling. Ideas to significantly improve the sensitivity of laser search is proposed [29].

bound from HB star cooling can be avoided. This, combined with the argument from SN1987A, leads to the so-called “hadronic axion window” at $F_a \sim 10^6$ GeV ($m_a \sim 1$ eV) where constraints from stars are absent [19, 20]. (In the DFSZ model, the axion-electron interaction induces rapid star cooling for this value of F_a , hence there is no such an window.) However, recent cosmological data disfavor such a scenario, because thermally produced axions contribute as hot dark matter component of the Universe. (See Section 3.2.2).

Long range forces Since axion is very light, it can mediate macroscopic long range forces [30]. Due to the CP-odd nature of the axion, the coherent interaction (or monopole-monopole interaction) between macroscopic objects are suppressed. Instead, searches for monopole-dipole interactions provide limits on the axion-nucleon and axion-electron coupling [31, 32], although it is still far from the prediction of QCD axion.⁴

To summarize, the best limit on the PQ scale and the axion mass comes from astrophysical arguments. Future axion helioscope experiment may reach a realistic parameters predicted in the QCD axion model. The cavity experiment will also be sensitive to the axion DM : if axion is the dominant component of DM, the ADMX will detect its signatures for realistic values of F_a . Some novel ideas are also proposed for detecting the axion DM for $F_a \gtrsim 10^{15}$ GeV [34].

3 Axion cosmology

3.1 Evolution of PQ scalar

The Peccei-Quinn (PQ) scalar field has the following lagrangian:

$$\mathcal{L} = \frac{1}{2}|\partial_\mu\phi|^2 - V_{\text{eff}}(\phi, T), \quad (5)$$

where $V(\phi, T)$ is the effective potential at temperature T and given by

$$V_{\text{eff}} = \frac{\lambda}{4}(|\phi|^2 - \eta^2)^2 + \frac{\lambda}{6}T^2|\phi|^2. \quad (6)$$

The above lagrangian is invariant under the global $U(1)_{\text{PQ}}$ transformation, $\phi \rightarrow \phi e^{i\alpha}$ with α constant. At high temperature $T > T_c \equiv \sqrt{3}\eta$, the potential has the minimum at $\phi = 0$ and the vacuum has the $U(1)_{\text{PQ}}$ symmetry (Figure 1). However, as the cosmic temperature decreases, the vacuum with $\phi = 0$ becomes unstable and the PQ scalar ϕ obtains vacuum expectation value $|\phi| = \eta$ (Figure 1). Thus, $U(1)_{\text{PQ}}$ symmetry is spontaneously broken at $T < T_c$. The axion a is a Nambu-Goldstone boson associated with this spontaneous symmetry breaking and corresponds to the phase direction of the PQ scalar as

$$\phi = |\phi|e^{i\theta_a} = |\phi|e^{ia/\eta}. \quad (7)$$

Since the phase direction is flat in the potential 6, the axion is massless at this point.

⁴ It is argued that searches for monopole-monopole force combined with star cooling constraints give stronger constraint [33].

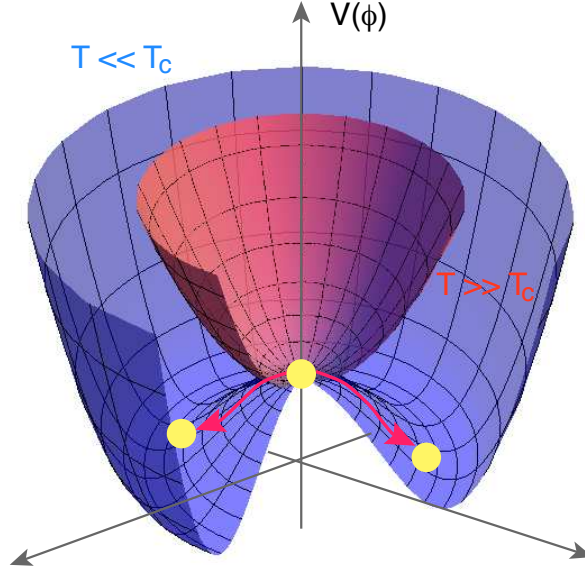


Figure 1: Potential of the PQ scalar.

When the $U(1)_{\text{PQ}}$ symmetry is spontaneously broken, one-dimensional topological defects called axionic strings are formed. After formation the axionic string networks evolve by emitting axions and follow the scaling solution. The emission of axions from the strings and its contribution to the present density is described in Section 3.3.1.

When the cosmic temperature further decreases and becomes comparable to the QCD scale Λ ($\simeq 0.1$ GeV), the axion obtains its mass through the QCD non-perturbative effect. Then, the axion potential is written as

$$V(a) = \frac{m_a^2 \eta^2}{N_{\text{DW}}^2} \left(1 - \cos \frac{N_{\text{DW}} a}{\eta} \right), \quad (8)$$

where m_a is the mass of the axion. Here N_{DW} is called the domain wall number which is a model-dependent integer related to the color anomaly. The axion mass m_a depends on the temperature and it was first calculated in References [36]. More recently, Wantz and Shellard [37] obtained the temperature dependence of m_a using the interacting instanton

liquid model [38]. They gave a simple approximation in the form of the power-law as

$$m_a(T) = \begin{cases} 4.05 \times 10^{-4} \frac{\Lambda^2}{F_a} \left(\frac{T}{\Lambda}\right)^{-3.34} & T > 0.26\Lambda, \\ 3.82 \times 10^{-2} \frac{\Lambda^2}{F_a} & T < 0.26\Lambda, \end{cases} \quad (9)$$

where $\Lambda \simeq 400\text{MeV}$ and F_a is the axion decay constant given by $F_a = \eta/N_{\text{DW}}$. The axion potential 8 explicitly breaks $U(1)_{\text{PQ}}$ symmetry into its subgroup $Z_{N_{\text{DW}}}$ and has degenerated minima (vacua) at $a = 0, 2\pi/N_{\text{DW}}, \dots, 2\pi(N_{\text{DW}} - 1)/N_{\text{DW}}$. When the Hubble parameter H becomes comparable to the axion mass m_a , the axion starts to roll down to one of the minima. Since the axion field settles into different minima in different places of the Universe, domain walls are formed between different vacua. These domain walls attach the axionic strings. For $N_{\text{DW}} = 1$ the domain walls are disk-like objects whose boundaries are axionic strings and collapse by their tension. On the other hand, the string-domain wall networks are very complicated for $N_{\text{DW}} \geq 2$ and dominate the Universe soon after their formation, which causes a serious cosmological difficulty called domain wall problem. More details about the axion domain walls are found in Sections 3.3.2 and 3.3.3.

3.2 Abundance of the axion

3.2.1 Cold axion

The axion field starts to oscillate when the cosmic expansion rate H becomes comparable to the axion mass m_a . Using Equation 9, the condition $m_a(T_1) = 3H(T_1)$ leads to

$$T_1 = 0.98 \text{ GeV} \left(\frac{F_a}{10^{12}\text{GeV}} \right)^{-0.19} \left(\frac{\Lambda}{400\text{MeV}} \right). \quad (10)$$

The oscillation of the coherent field a is described by the equation of motion,

$$\ddot{a} + 3\frac{\dot{R}}{R}\dot{a} + m^2(T)a = 0, \quad (11)$$

where R is the scale factor. From Equation 11 we get

$$\dot{\rho}_a = -3\frac{\dot{R}}{R}\dot{a}^2 + \dot{m}_a m_a a^2, \quad (12)$$

where $\rho_a (= \dot{a}^2/2 + m_a^2 a^2/2)$ is the axion energy density. By averaging the above equation over an oscillation ($\langle \dot{a} \rangle = 0$ and $\langle m_a^2 a^2 \rangle = \rho_a$), it is found that $\rho_a R^3/m_a$ is invariant under

adiabatic condition $m_a \gg H$. Thus, we obtain the present axion number to entropy ratio as

$$Y_a^{(\text{cold})} = \frac{n_{a,0}}{s_0} = \beta \left(\frac{\rho_a/m_a}{s} \right)_{T=T_1}, \quad (13)$$

where s is the entropy density and s_0 is its present value. Here β is the correction factor taking into account that the adiabatic condition ($m_a \gg H$) is not satisfied at the beginning of the oscillation. The correction factor was calculated by [39] which gives $\beta = 1.85$. Thus, the present axion density is given by [40]

$$\Omega_a h^2 = 0.18 \theta_1^2 \left(\frac{F_a}{10^{12} \text{GeV}} \right)^{1.19} \left(\frac{\Lambda}{400 \text{MeV}} \right), \quad (14)$$

where h is the present Hubble parameter in units of 100km/s/Mpc. Here $\theta_1 = a_1/\eta$ is the initial angle at onset of oscillation. When the PQ symmetry is spontaneously broken after inflation, θ_1 is random in space and hence we should replace θ_1^2 by its spatial average, i.e. $\langle \theta_1^2 \rangle = \pi^2/3 \times c_{\text{anh}}$, where $c_{\text{anh}} (\simeq 2)$ is the anharmonic correction [40, 41]. On the other hand, if PQ symmetry is broken before or during inflation, θ_1 takes the same value in the whole observable Universe. Then, θ_1 is considered as a free parameter.

The density of the coherent axion oscillation cannot exceed the present DM density of the Universe determined from the observations of cosmic microwave background (CMB), $\Omega_{\text{CDM}} h^2 = 0.11$. This gives the following upper bound on the axion decay constant:

$$F_a \lesssim 1.4 \times 10^{11} \text{ GeV}, \quad (15)$$

when the PQ symmetry is broken after inflation. For the case of PQ symmetry breaking before or during inflation, see Section 3.3.⁵

3.2.2 Hot axion

Axions are also produced in high-temperature plasma [43, 44]. The abundance of such hot axions in the KSVZ model, in terms of the number-to-entropy ratio $Y_a \equiv n_a/s$, was estimated recently in [44] :

$$Y_a^{(\text{hot})} \simeq 1.9 \times 10^{-3} g_s^6 \ln \left(\frac{1.501}{g_s} \right) \left(\frac{10^{12} \text{GeV}}{F_a} \right)^2 \left(\frac{T_R}{10^{10} \text{GeV}} \right), \quad (16)$$

⁵ Notice that Equation 14 assumes no late-time entropy production after the QCD phase transition. If there is a late-time entropy production by decaying particles, the abundance is reduced and upper bound on the PQ scale is relaxed [42].

where T_R denotes the reheating temperature after inflation. Notice that the above expression applies for $T_R < T_D$ with

$$T_D \simeq 9.6 \times 10^6 \text{ GeV} \left(\frac{F_a}{10^{10} \text{ GeV}} \right)^{2.246}. \quad (17)$$

Otherwise, axions are thermalized at $T > T_D$ and decouple at $T \simeq T_D$. Then the relic abundance is given by $Y_a^{(\text{hot})} = 0.28/g_*(T_D)$ ($\simeq 2.6 \times 10^{-3}$ for $g_*(T_D) = 106.75$).

The above calculations were carried out in quark-gluon plasma. For small $F_a (\lesssim 10^7 \text{ GeV})$, the axion decoupling may occur after the QCD phase transition. The decoupling temperature and the resultant axion abundance in such a case were estimated in [19, 45] by taking account of the axion-pion interaction. Since the axion mass is given by $m_a \gtrsim 0.6 \text{ eV}$ for $F_a \lesssim 10^7 \text{ GeV}$, it contributes to the hot dark matter and such a contribution is restricted from cosmological observations. According to recent results [46], the constraint reads $m_a < 0.91 \text{ eV}$ assuming massless neutrinos and $m_a < 0.72 \text{ eV}$ after marginalizing over the neutrino mass. This closes a hadronic axion window (see Section 2.2).

3.3 PQ symmetry breaking after inflation

Cosmological consequences of axions are different depending on whether the PQ symmetry is broken after inflation or not. When the symmetry breaking takes place after inflation, topological defects like strings and domain walls are formed in the course of evolution of the PQ scalar as shown in Section 3.1. On the other hand, if the PQ symmetry is broken before or during inflation, the produced strings are diluted away and the field value of the axion is the same in the whole observable Universe. Thus, the axion settles into the same minimum when it acquires the mass at the QCD scale, and hence domain walls are not formed. So no domain wall problem exists. However, in this case, the axion (which already exists during inflation) obtains large fluctuations and produces isocurvature density perturbations which are stringently constrained by the CMB observations. In this section, we first consider the case where the PQ symmetry breaking occurs after inflation and see cosmological consequences the axionic strings and domain walls.

3.3.1 Axionic strings

When the $U(1)_{\text{PQ}}$ symmetry is spontaneously broken, one-dimensional topological defects called axionic strings are produced. Since the $U(1)_{\text{PQ}}$ is a global symmetry, the axionic string is a global one. Unlike local strings which eventually lose their energy by emitting gravitational waves, the emission of the Nambu-Goldstone bosons, i.e. axions is a dominant energy loss process for axionic strings. After formation the axionic string networks evolve by emitting axions and follow a scaling solution in which the energy density of the string networks ρ_{str} is written as

$$\rho_{\text{str}} = \xi \frac{\mu}{t^2}, \quad (18)$$

where ξ is the length parameter which is constant in the scaling regime and μ is the string tension given by

$$\mu = \pi F_a^2 \ln \left(\frac{t/\sqrt{\xi}}{\delta_s} \right), \quad (19)$$

where $\delta_s = 1/\sqrt{\lambda}\eta$ is the width of the strings. ξ represents average number of infinite strings in a volume t^3 (\sim horizon volume) and is determined by numerical simulations [47, 48, 49, 50]. Figure 2 shows the recent simulation [50] and the evolution of the length parameter ξ is shown in Figure 3. For the axionic string networks, $\xi \simeq 0.7 - 1.0$.

The axions emitted from the axionic string networks give a significant contribution to the present matter density of the Universe. This was first pointed out by Davis [51] [see also [52, 53]]. The axion density due to the axionic strings depends on the energy spectrum of the emitted axions. Davis and co-workers claimed that the energy spectrum has a sharp peak at the horizon scale [51, 52, 53]. On the other hand, Sikivie and co-workers [54, 55, 56] insisted that the spectrum is proportional to $1/k$ (k : axion momentum). Because the present axion density is given by $\rho_a = m_a(0)n_a$, it is crucial how many axions are produced from the strings. Since smaller number of axions are emitted for the $1/k$ spectrum, the present density of the axions is less important than that for Davis's spectrum. This controversy was solved by field theoretical lattice simulations [48, 50] which showed that the spectrum is sharply peaked around the horizon scale and exponentially suppressed at higher momenta as seen in Figure 4. Using this spectrum, the mean reciprocal comoving momentum of the emitted axions $\langle 1/k \rangle$ which is important in calculating the axion number

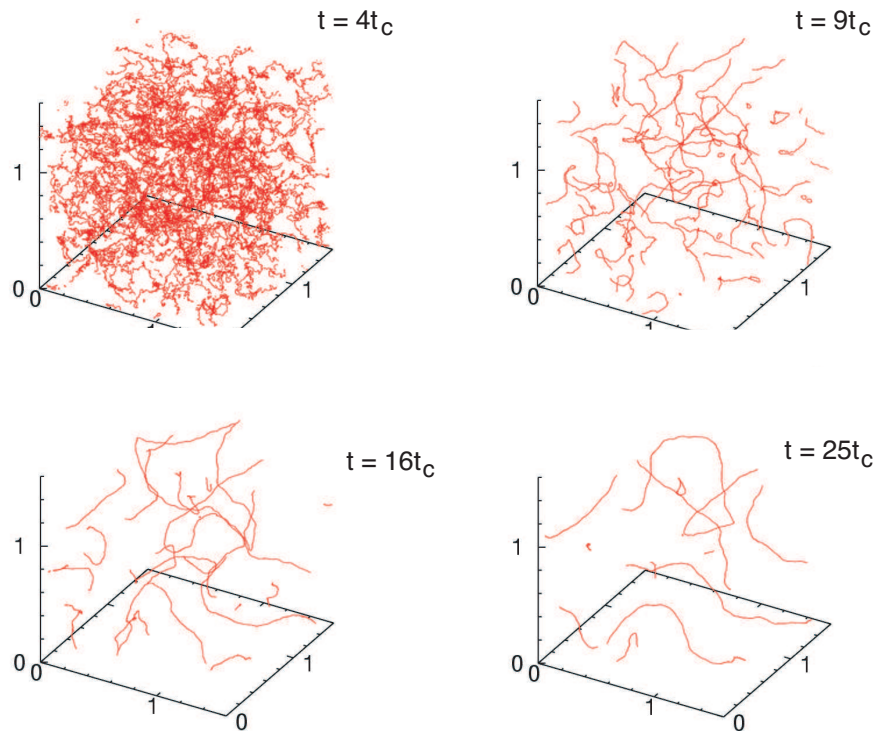


Figure 2: Evolution of the axionic string networks from the simulation [50]. The panels show the time slices at $t = 4t_c$, $9t_c$, $16t_c$ and $25t_c$ where t_c is the cosmic time corresponding to the critical temperature T_c . The spatial scale shows a comoving length in unit of the horizon size at $t_{\text{end}} = 25t_c$.

density is estimated as [50]

$$\langle 1/k \rangle R(t) \simeq 0.23 \frac{t}{2\pi}, \quad (20)$$

where $(2\pi)/t$ is the momentum corresponding to the horizon scale. Thus, the present axion density due to the axionic strings is estimated as

$$\Omega_{a,\text{str}} h^2 = 2.0 \, \xi \left(\frac{F_a}{10^{12} \text{GeV}} \right)^{1.19} \left(\frac{\Lambda}{400 \text{MeV}} \right). \quad (21)$$

Notice that the string contribution is larger than the coherent oscillation given in Equation 14.

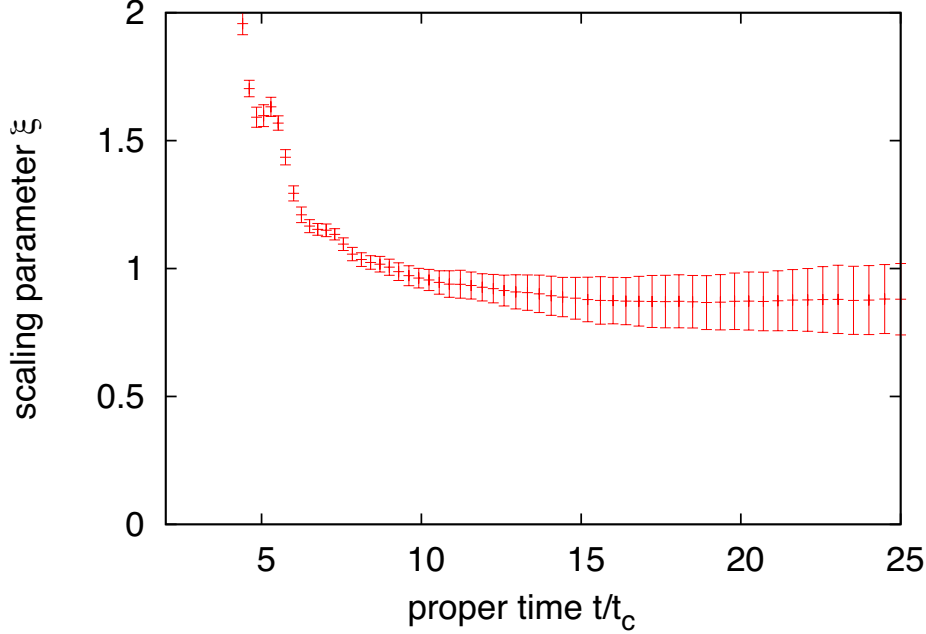


Figure 3: Time evolution of the length parameter ξ from the simulation [50].

3.3.2 Axionic domain walls with $N_{\text{DW}} = 1$

Around the QCD scale, the axion acquires mass through QCD instanton effect and the axion potential is given by Equation 8. Since the potential has N_{DW} discrete minima and the axion settles down to one of the minima, the Universe is divided into many domains with different vacua and domain walls are formed separating those domains. Around an axionic string, the phase of the PQ scalar ($\theta_a = a/\eta$) rotates 2π , so N_{DW} domain walls attach each string. The cosmological evolutions of the string-domain wall networks are quite different between $N_{\text{DW}} = 1$ and $N_{\text{DW}} \geq 2$.

First, let us consider the case of $N_{\text{DW}} = 1$. The domain walls with $N_{\text{DW}} = 1$ are disk-like objects bounded by strings and collapse by their tension. Thus, the string-domain wall networks are unstable for $N_{\text{DW}} = 1$ and they decay soon after formation. This was confirmed in 2-dimensional [57] and 3-dimensional [58] numerical simulations. In Figure 5 the evolution of the domain walls is shown and it is seen that the string-domain wall networks decay and disappear in the Universe. So in this case there is no domain wall problem.

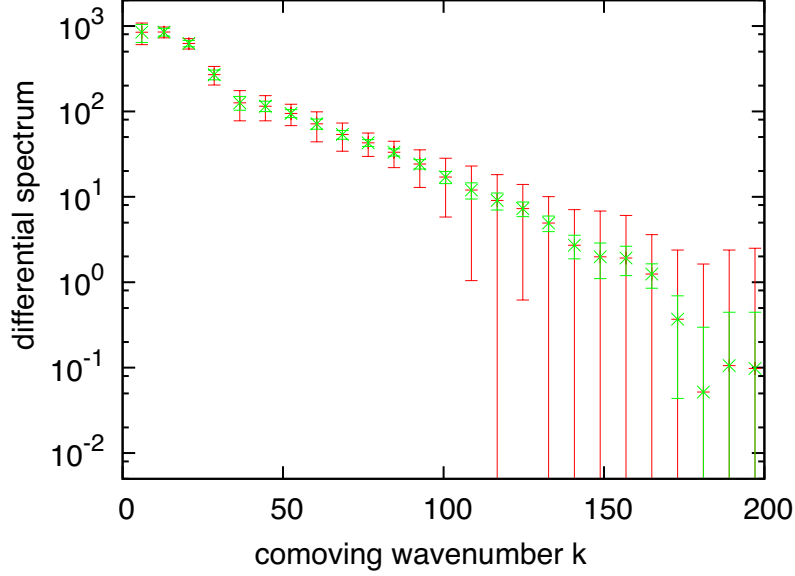


Figure 4: Differential energy spectrum of radiated axions between $t_1 = 12.25t_c$ and $t_2 = 25t_c$. Green (red) bars correspond to statistical errors alone (statistical and systematic errors). The comoving wavenumber k is in units of $(2t_c)^{-1}$. Note that the horizon scale corresponds to $k \sim 3$. The scale in y -axis is arbitrary.

However, a large number of axions are produced in the decay of the string-domain wall networks and they give a significant contribution to the present matter density of the Universe. Similarly to axions from the axionic strings, there has been controversy about the spectrum of the axions emitted from domain walls. In [59] it was found that the spectrum has a peak around m_a which is the width of the domain walls, so axions from domain walls are mildly relativistic. On the other hand, the authors in [60, 61] claimed that the mean axion energy is larger than that in [59] by a factor 20. This conclusion comes from the reasoning that the energy of the domain walls is converted into strings which emits axion with spectrum proportional to $1/k$ following [54, 55, 56]. The recent 3-dimensional lattice simulation [58] settled this problem and showed that the axions produced in the string-wall decay are mildly relativistic with mean momentum $\langle k \rangle / R \simeq 3m_a$ which is consistent with [59]. The energy density of the axions today is then estimated as

$$\Omega_{a,\text{wall}} h^2 = (5.8 \pm 2.8) \left(\frac{F_a}{10^{12} \text{GeV}} \right)^{1.19} \left(\frac{\Lambda}{400 \text{MeV}} \right). \quad (22)$$

Comparing to the contributions from the coherent oscillation (Equation 14) and strings (Equation 21), it is found that the axions from the string-wall networks gives a dominate contribution to the present DM density.

The total density of the cold axions is given by

$$\Omega_{a,\text{tot}} h^2 = (8.4 \pm 3.0) \left(\frac{F_a}{10^{12} \text{GeV}} \right)^{1.19} \left(\frac{\Lambda}{400 \text{MeV}} \right), \quad (23)$$

where we take $\xi = 1.0 \pm 0.5$ in Equation 21. Thus we obtain the following constraint on the axion decay constant:

$$F_a \lesssim (2.0 - 3.8) \times 10^{10} \text{ GeV}. \quad (24)$$

3.3.3 Axionic domain walls with $N_{\text{DW}} \geq 2$

The wall-string networks with $N_{\text{DW}} \geq 2$ have complicated structures and do not decay contrary to the walls with $N_{\text{DW}} = 1$. After formation, the long-lived wall-string networks evolve into the scaling regime as shown in the simulations [62, 57]. The domain wall density is written as

$$\rho_{\text{wall}} = \mathcal{A} \frac{\sigma_{\text{wall}}}{t}, \quad (25)$$

where σ_{wall} is the wall tension given by $\sigma_{\text{wall}} = 9.23 m_a F_a^2$. Here \mathcal{A} is the surface parameter which becomes constant in the scaling regime. Since the total cosmic density decreases as $1/t^2$, the domain walls soon dominate the Universe, which conflicts the standard cosmology.

To solve the domain wall problem, one can introduce an additional term in the axion potential which explicitly breaks the $Z_{N_{\text{DW}}}$ symmetry,

$$\delta V = -\Xi \eta^3 (\phi e^{i\delta} + \text{h.c.}), \quad (26)$$

where Ξ is a small parameter describing the size of the explicit $Z_{N_{\text{DW}}}$ breaking and δ is the phase. This term is called a “bias” and lifts the degenerated vacua so that the potential has a unique minimum at $a \simeq 0$. The energy difference between the neighboring vacuum produces a volume pressure and makes the domain walls accelerate toward the false vacuum. Thus, the false vacuum regions shrink and the domain walls annihilate each other. Let us estimate the decay epoch of the string-wall networks with bias. The

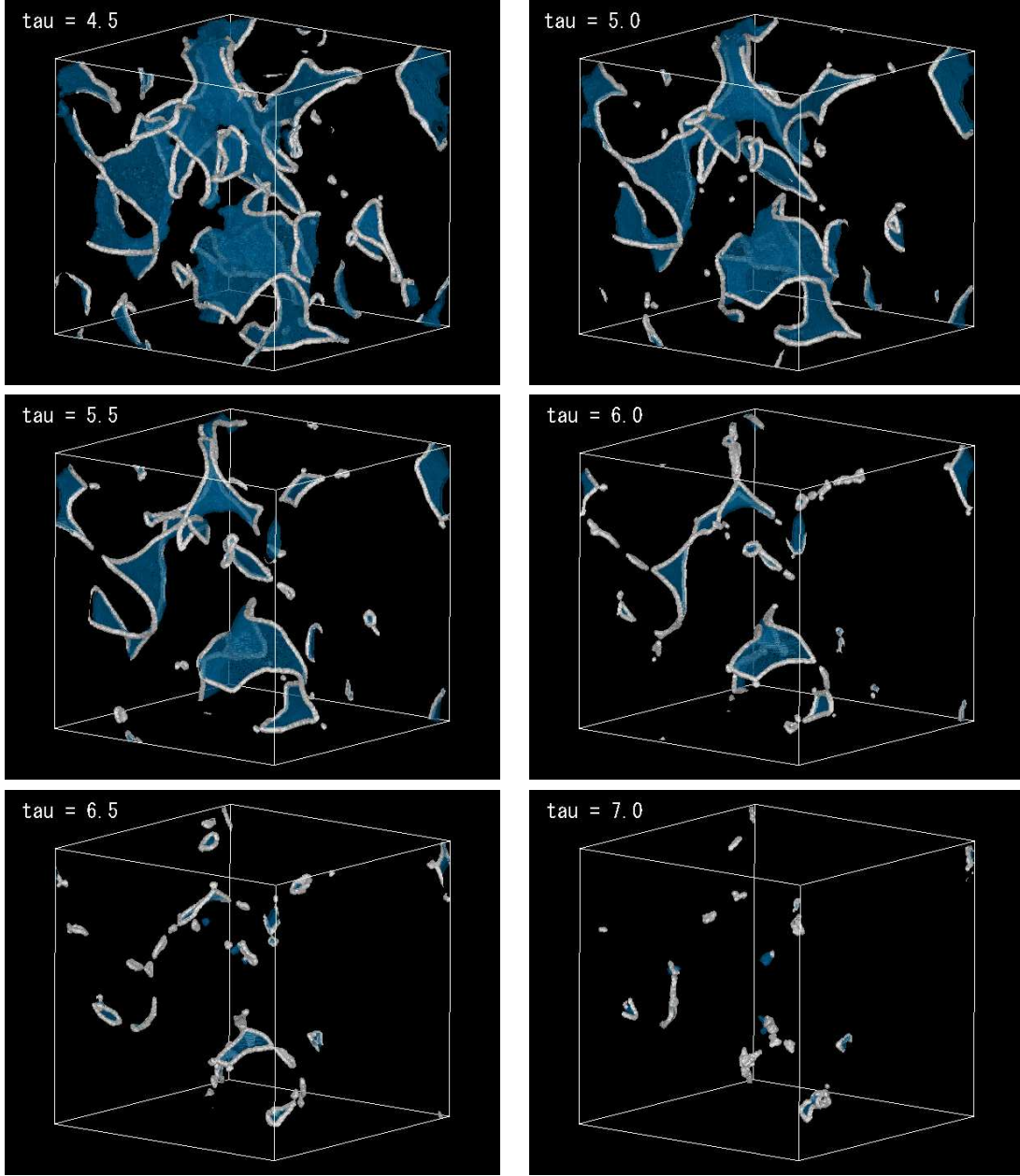


Figure 5: Evolution of the string-domain wall networks for $N_{\text{DW}} = 1$. The white lines correspond to the position of strings, while the blue surfaces correspond to the position of the center of domain walls. “tau” in each panel is the conformal time which is related to the cosmic time as $\text{tau} = \sqrt{t\eta}$.

pressure due to the bias term is roughly given by the difference of neighboring vacua which is $p_V \sim 4\pi\Xi\eta^4/N_{\text{DW}}$. On the other hand, the pressure from the surface tension which straightens the wall up to the horizon scale is $p_T \sim \sigma_{\text{wall}}/t$. The domain walls collapse when $p_V \sim p_T$, so the decay time t_{dec} is estimated as

$$t_{\text{dec}} \sim \frac{\sigma_{\text{wall}}}{\Xi\eta^4/N_{\text{DW}}}. \quad (27)$$

Using $\sigma_{\text{wall}} \sim m_a\eta^2/N_{\text{DW}}^2$ we can write the above equation as

$$t_{\text{dec}} = \alpha \frac{m_a}{\Xi\eta^2 N_{\text{DW}}}, \quad (28)$$

where $\alpha \simeq 18$ is determined by the numerical simulation [57].

The string-wall networks continuously emit axions until they decay at t_{dec} . The spectrum of the emitted axions has a peak around the momentum scale determined by the mass of axion as shown in Figure 6 and the mean momentum of the axions ϵ_a is estimated as $\epsilon_a = \langle k \rangle / R \simeq 3m_a$. This is the same as the case for $N_{\text{DW}} = 1$. Then we can obtain the present density of axions from the string-wall networks,

$$\Omega_{a,\text{wall}} h^2 \simeq 0.3 \mathcal{A} N_{\text{DW}}^{-3/2} \left(\frac{\Xi}{10^{-52}} \right)^{-1/2} \left(\frac{F_a}{10^{10} \text{GeV}} \right)^{-1/2}. \quad (29)$$

Since the long-lived walls produce more axions than the wall with $N_{\text{DW}} = 1$, the cosmological constraint is more stringent as seen below.

Gravitational waves are also produced from the string-wall networks. Since the characteristic length scale of the domain walls is the Hubble time $\sim t$, the quadruple moment Q_{ij} of the system is estimated as $Q_{ij} \sim \rho_{\text{wall}} t^3 t^2 \sim \sigma_{\text{wall}} \mathcal{A} t^4$. Using the quadrupole formula the energy of the gravitational waves is $E_{\text{gw}} \sim G \mathcal{A}^2 \sigma_{\text{wall}}^2 t^3$. Thus we can write the energy density of the produced gravitational waves as

$$\rho_{\text{gw}} = \epsilon_{\text{gw}} G \mathcal{A}^2 \sigma_{\text{wall}}^2, \quad (30)$$

where ϵ_{gw} is the efficiency of gravitational waves and $\epsilon_{\text{gw}} \simeq 5$ from the simulation [63]. The present density of the gravitational waves is calculated as

$$\Omega_{\text{gw}} h^2 \simeq 10^{-19} \mathcal{A}^2 N_{\text{DW}}^{-6} \left(\frac{\Xi}{10^{-52}} \right)^{-2} \left(\frac{F_a}{10^{10} \text{GeV}} \right)^{-4}. \quad (31)$$

The amplitude of gravitational waves produced by the domain walls is too small to be detected in the current and future-planned experiments for allowed values of Ξ and F_a (see below).

Let us examine whether we have a consistent scenario with $N_{\text{DW}} \geq 2$ or not. First the cosmic density of the cold axions should not exceed the CDM density measured by the CMB observations which gives

$$\Omega_{a,\text{tot}} = \Omega_a + \Omega_{a,\text{str}} + \Omega_{a,\text{wall}} < 0.11. \quad (32)$$

Second, the bias term shifts the minimum of the axion potential by

$$\bar{\theta} = \frac{\langle a \rangle}{\eta} = \frac{2\Xi N_{\text{DW}}^3 F_a^2 \sin \delta}{m_a^2 + 2\Xi N_{\text{DW}}^2 F_a^2 \cos \delta}, \quad (33)$$

which violates CP. From the experimental upper bound on NEDM [5], θ should satisfy

$$\bar{\theta} < 0.7 \times 10^{-11}, \quad (34)$$

which leads to the constraints on Ξ and F_a through Equation 33. Finally, we have the astrophysical constraint from SN1987A, $F_a > 4 \times 10^8$ GeV. In Figure 7 these constraints are shown. If the phase of the bias term δ is $O(1)$, there is no allowed region and the allowed region appears for $\delta \lesssim 10^{-2}$. Therefore, when the PQ symmetry is broken after inflation, the axion models with $N_{\text{DW}} \geq 2$ are excluded unless the phase of the bias term is fine-tuned.

3.4 PQ symmetry breaking before/during inflation

If the PQ symmetry is broken before or during inflation, inflation expands a domain with some PQ phase θ_a to the size larger than the present observable Universe. Thus, there are no topological defects and hence no axions from the axionic domain walls and strings in the Universe. The present axion density comes from the coherent oscillation and is given by Equation 14 :

$$\Omega_a h^2 = 0.18 \theta_a^2 \left(\frac{F_a}{10^{12} \text{GeV}} \right)^{1.19} \left(\frac{\Lambda}{400 \text{MeV}} \right), \quad (35)$$

where θ_a is constant in the whole observable Universe and considered as a free parameter. This leads to the upper bound on the axion decay constant,

$$F_a < 6.6 \times 10^{11} \theta_a^{-1.68} \text{ GeV}. \quad (36)$$

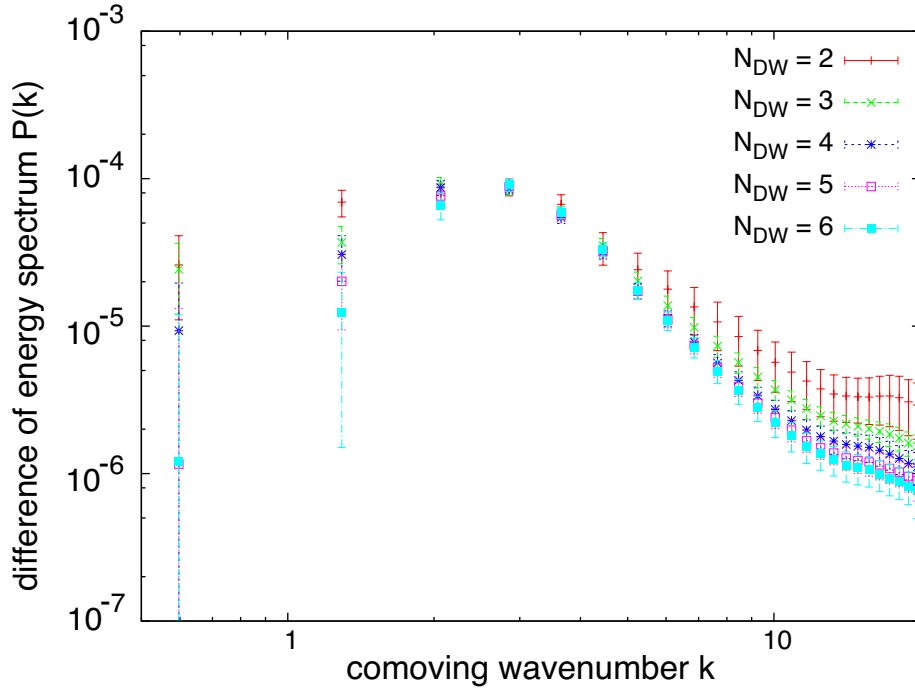


Figure 6: The spectra of axions produced by string-wall networks for various values of N_{DW} in the numerical simulation [63]. The spectra shown in this figure are the difference of power spectra evaluated at two different time steps $t_1 = 49\eta^{-1}$ and $t_2 = 400\eta^{-1}$. The momentum scale corresponding to the axion mass is given by $k \sim R(t_2)m_a \sim 2$.

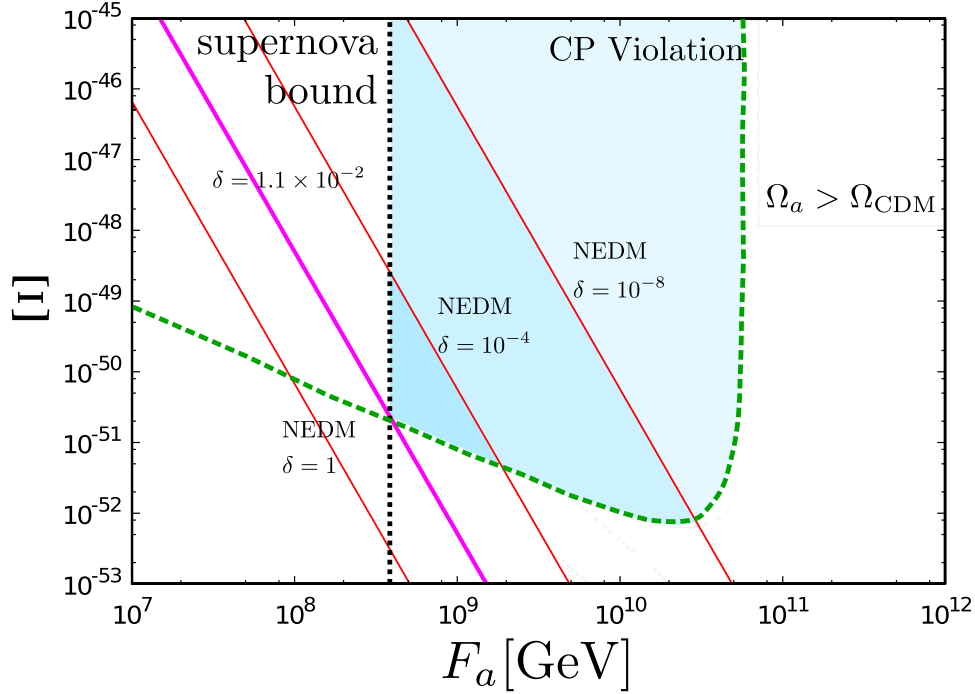


Figure 7: The various observational constraints in the parameter space of F_a and Ξ . The green dashed-line represents the parameter region satisfying $\Omega_{a,\text{tot}} < \Omega_{\text{CDM}}$, and the region below this line is excluded since the relic abundance of axions exceeds the cold dark matter abundance observed today. The vertical dotted-line represents the bound from the observation of supernova 1987A. The red solid-lines represent the NEDM bound for $\delta = 1, 10^{-4}$, and 10^{-8} . The region above these lines is excluded since it leads to an experimentally unacceptable amount of CP-violation. The pink line represents the NEDM bound for the critical value $\delta = 1.1 \times 10^{-2}$. There are still allowed regions if the value of δ is smaller than this critical value. In this figure, we fixed other parameters as $N_{\text{DW}} = 6$, $\epsilon_a = 1.5$ and $\mathcal{A} = 2.6$.

Notice that F_a much larger than 10^{12} GeV is allowed for $\theta_a \ll 1$.

During inflation the axion field obtains the fluctuations whose power spectrum is given by

$$\mathcal{P}_{\delta a} = \frac{H_{\text{inf}}^2}{4\pi^2}. \quad (37)$$

Here the power spectrum $\mathcal{P}_{\delta a}$ is defined by

$$\langle \delta a(\vec{k}) \delta a(\vec{k}') \rangle = (2\pi)^3 \delta^{(3)}(\vec{k} + \vec{k}') \frac{2\pi^2}{k^3} \mathcal{P}_{\delta a}(k), \quad (38)$$

where $\delta a(\vec{k})$ is the Fourier component of $\delta a(\vec{x})$ and $\langle \cdots \rangle$ denotes the ensemble average. Here notice that the fluctuations of the axion field also give a contribution to the mean energy density. Using $\langle \delta a^2(\vec{x}) \rangle \simeq H_{\text{inf}}^2/4\pi^2$ derived from Equations 37 and 38, Equation 35 should be replaced by

$$\Omega_a h^2 = 0.18 \left[\theta_a^2 + \left(\frac{H_{\text{inf}}}{2\pi F_a} \right)^2 \right] \left(\frac{F_a}{10^{12} \text{GeV}} \right)^{1.19} \left(\frac{\Lambda}{400 \text{MeV}} \right). \quad (39)$$

When the axion fluctuations are larger than the homogeneous value $F_a \theta_a$, the cosmic axion density is dominated by the fluctuations and the constraint on F_a and H_{inf} is given by [41]

$$H_{\text{inf}} < 5.0 \times 10^{12} \text{GeV} \left(\frac{F_a}{10^{12} \text{GeV}} \right)^{0.41} \quad \text{for} \quad F_a < \frac{H_{\text{inf}}}{2\pi \theta_a}. \quad (40)$$

On the other hand, for $F_a > H_{\text{inf}}/2\pi \theta_a$, Equation 36 is valid.

The axion fluctuations turn into isocurvature density perturbations of the axions when the axions acquire mass at the QCD scale [64, 65, 66, 67, 68, 69, 41]. The definition of the axion isocurvature perturbations S_a is

$$S_a(\vec{x}) = 3(\zeta_a - \zeta), \quad (41)$$

where ζ_a and ζ are the curvature perturbations on the uniform density slices of the axion and the total matter, respectively. According to δN formalism [70, 71] the axion energy density $\rho_a(\vec{x})$ on the uniform density slice of the total matter is given by $\rho_a(\vec{x}) = \bar{\rho}_a e^{S_a}$ where $\bar{\rho}_a$ is the mean density of the axion. Since $\rho_a(\vec{x}) \propto (a_i + \delta a(\vec{x}))^2$ with $a_i = F_a \theta_a$,

$$e^{S_a} = 1 + 2 \frac{\delta a(\vec{x})}{a_*^2} + \frac{\delta a^2(\vec{x}) - \langle \delta a^2 \rangle}{a_*^2}, \quad (42)$$

where $a_*^2 = a_i^2 + \langle \delta a^2 \rangle$. Define r as the ratio of the mean axion density $\bar{\rho}_a$ to the total CDM density $\bar{\rho}_{\text{CDM}}$, the CDM density on the uniform density slice of the total matter is

$$\rho_{\text{CDM}}(\vec{x}) = \bar{\rho}_{\text{CDM}} \left[(1 - r) + r e^{S_a} \right]. \quad (43)$$

Thus, we obtain the CDM isocurvature density perturbations S_{CDM} as

$$\begin{aligned} S_{\text{CDM}} &= \ln \left(\frac{\rho_{\text{CDM}}(\vec{x})}{\bar{\rho}_{\text{CDM}}} \right) \\ &= 2r \frac{F_a \theta_a \delta a}{a_*^2} + r \frac{\delta a^2 - \langle \delta a^2 \rangle}{a_*^2}. \end{aligned} \quad (44)$$

The energy fraction of the axion in CDM is given by

$$r = 1.6 \left[\theta_a^2 + \left(\frac{H_{\text{inf}}}{2\pi F_a} \right)^2 \right] \left(\frac{F_a}{10^{12} \text{GeV}} \right)^{1.19} \left(\frac{\Lambda}{400 \text{MeV}} \right). \quad (45)$$

The power spectrum of the CDM isocurvature perturbations is written as

$$\langle S_{\text{CDM}}(\vec{k}) S_{\text{CDM}}(\vec{k}') \rangle = (2\pi)^3 \delta^{(3)}(\vec{k} + \vec{k}') \frac{2\pi^2}{k^3} \mathcal{P}_{S_{\text{CDM}}}(k), \quad (46)$$

$$\mathcal{P}_{S_{\text{CDM}}} = 4r^2 \frac{(H_{\text{inf}}/2\pi)^2}{(F_a \theta_a)^2 + (H_{\text{inf}}/2\pi)^2}, \quad (47)$$

The amplitude of the isocurvature perturbations is stringently constrained by the CMB observations [72, 73, 74, 75, 76, 77, 78, 79]. The analysis using WMAP 7 year data [80] finds $\alpha = \mathcal{P}_{S_{\text{CDM}}}(k_*)/\mathcal{P}_\zeta(k_*) < 0.15$ at the reference scale $k_* = 0.002 \text{Mpc}^{-1}$ where \mathcal{P}_ζ is the power spectrum of the curvature perturbations. This limit is translated into the constraint on F_a and H_{inf} as

$$\left[\theta_a^2 + \left(\frac{H_{\text{inf}}}{2\pi F_a} \right)^2 \right] \left(\frac{H_{\text{inf}}}{2\pi F_a} \right)^2 \left(\frac{F_a}{10^{12} \text{GeV}} \right)^{2.38} < 3.6 \times 10^{-11}. \quad (48)$$

Here we have used $\mathcal{P}_\zeta(k_*) = 2.43 \times 10^{-9}$.

Although the axion fluctuation δa is Gaussian, δa^2 -term in Equation 44 is not Gaussian and hence leads to non-Gaussianity in the isocurvature perturbations in CDM [81, 82, 83, 84, 85, 86, 87, 88]. The non-Gaussianity clearly appears in the bispectrum $B(k_1, k_2, k_3)$ of the isocurvature perturbations which is defined as [82]

$$\langle S_{\text{CDM}}(\vec{k}_1) S_{\text{CDM}}(\vec{k}_2) S_{\text{CDM}}(\vec{k}_3) \rangle = (2\pi)^3 B_{S_{\text{CDM}}}(k_1, k_2, k_3) \delta^{(3)}(\vec{k}_1 + \vec{k}_2 + \vec{k}_3), \quad (49)$$

$$B_{S_{\text{CDM}}}(k_1, k_2, k_3) = f_S \left(\frac{(2\pi^2)^2}{k_1^3 k_2^3} \mathcal{P}_{S_{\text{CDM}}}(k_1) \mathcal{P}_{S_{\text{CDM}}}(k_2) + (2 \text{ perms}) \right), \quad (50)$$

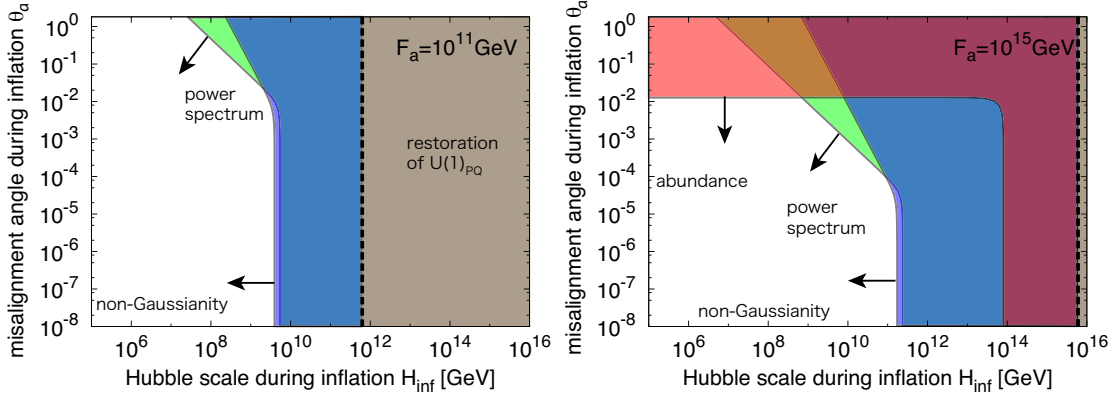


Figure 8: Constraints on axion isocurvature model in the $H_{\text{inf}}-\theta_a$ plane for $F_a = 10^{11}\text{GeV}$ (left panel) and $F_a = 10^{15}\text{GeV}$ (right panel). Shaded regions are excluded by cosmological considerations. At small θ_a , the constraint on H_{inf} from the non-Gaussianity is slightly better than one from the power spectrum. When $H_{\text{inf}}/2\pi > F_a$ the PQ symmetry restores during inflation.

where f_S is the non-linearity parameter which is given by $1/(2r)$ for the isocurvature perturbations produced by the axion fluctuations.⁶

At present CMB is the best probe of non-Gaussianity in isocurvature perturbations and it was investigated by using WMAP 3 year data [89] and more recently WMAP 7 year data [90]. The resultant 2σ constraint is

$$|f_{\text{NL}}^{S,SS}| = |\alpha^2 f_S| < 140, \quad (51)$$

from which we obtain the following constraint:

$$\left[\theta_a^2 + \left(\frac{H_{\text{inf}}}{2\pi F_a} \right)^2 \right] \left(\frac{H_{\text{inf}}}{2\pi F_a} \right)^4 \left(\frac{F_a}{10^{12}\text{GeV}} \right)^{3.56} < 2.5 \times 10^{-17}. \quad (52)$$

In Figure 8 the cosmological constraints on axion models are shown in the $H_{\text{inf}}-\theta_a$ plane.

4 Supersymmetry and axion

In this section we give a brief review on supersymmetric extension of the axion model. Since SUSY naturally solves the gauge hierarchy problem, we have a good motivation to

⁶The parameter f_S is related to $f_{\text{NL}}^{S,SS}$ in [88] through the relation $f_{\text{NL}}^{S,SS} = \alpha^2 f_S$. This is further related to $f_{\text{NL}}^{(\text{iso})}$ in [84] through $f_{\text{NL}}^{S,SS}/27 = (6/5)f_{\text{NL}}^{(\text{iso})}$.

consider the SUSY axion model. In extending the axion model into a SUSY framework, there are some non-trivial features which must be addressed carefully. First, in SUSY, there exists a flat direction in the PQ scalar potential in addition to the massless axion. This is due to the holomorphic property of the superpotential [91] : in the $U(1)_{\text{PQ}}$ transformation $\phi_j \rightarrow e^{i\alpha_j}\phi_j$, the rotation parameter α_j can be complex. Therefore, by taking α_j to be pure imaginary, the theory should be invariant under the scale transformation, which means that there is a flat direction in the scalar potential correspondingly and hence the PQ scalar is not stabilized. This argument breaks down under the SUSY breaking effect. Thus in order to stabilize the PQ scalar at an appropriate scale, we are forced to consider SUSY breaking and its effects on the structure of the scalar potential. Second, there appear very weakly coupled massive particles, saxion (scalar partner of axion) and axino (fermion partner of axion), which might have significant cosmological effects [92, 93].

4.1 Stabilization of the PQ scalar

In this subsection we show some explicit models of PQ scalar stabilization. We do not aim to make a complete list of stabilization mechanism, but rather show typical examples, which may be a good starting point for considering phenomenology of the SUSY axion model.

4.1.1 Model A

One of the simplest model for stabilizing the PQ scalar is described by the following superpotential :

$$W_{\text{PQ}} = \kappa X(\phi\bar{\phi} - \eta^2), \quad (53)$$

where X is a singlet superfield with no PQ charge, and ϕ ($\bar{\phi}$) is a PQ scalar with PQ charge $+1$ (-1), and κ is a constant taken to be real hereafter. The R -symmetry under which X has a charge $+2$ and $\phi, \bar{\phi}$ are singlet ensures this form of the superpotential. By taking into account the SUSY breaking effect, the (relevant portion of) scalar potential is given by

$$V = m_s^2|\phi|^2 + m_{\bar{s}}^2|\bar{\phi}|^2 + \kappa^2|\phi\bar{\phi} - \eta^2|^2 + \kappa^2|X|^2(|\phi|^2 + |\bar{\phi}|^2). \quad (54)$$

where m_s^2 and $m_{\bar{s}}^2$ represent soft SUSY breaking masses for ϕ and $\bar{\phi}$. PQ scalars are stabilized at $\langle\phi\rangle \sim \langle\bar{\phi}\rangle \sim \eta$ and $\langle X\rangle \sim 0$. To be more precise, X obtains a VEV of $\langle X\rangle \sim m_{3/2}/\kappa$, where $m_{3/2}$ denotes the gravitino mass, by taking account of the constant term in the superpotential ($W_0 = m_{3/2}M_P^2$) to cancel the cosmological constant. In this model, the saxion corresponds to the fluctuation around the VEVs of ϕ and $\bar{\phi}$ along the flat direction $\phi\bar{\phi} = \eta^2$, and it obtains a mass of soft SUSY breaking scale, which might be of the order of TeV. The axino (\tilde{a}) corresponds to the light combination of $\tilde{\phi}$ and $\tilde{\bar{\phi}}$, which are fermionic components of ϕ and $\bar{\phi}$, and obtains a mass of $m_{\tilde{a}} = \kappa\langle X\rangle \simeq m_{3/2}$. (The other combination mixes with \tilde{X} and gets a mass of $\kappa\eta$.)⁷

In order to solve the strong CP problem, we introduce a superpotential

$$W_{\text{KSVZ}} = k\phi Q\bar{Q}, \quad (55)$$

for the SUSY version of KSVZ axion model, where Q and \bar{Q} transforms as fundamental and anti-fundamental representations of $\text{SU}(3)_c$,⁸ and both have PQ charges of $-1/2$. On the other hand, in the SUSY version of DFSZ model, we introduce

$$W_{\text{DFSZ}} = \lambda \frac{\phi^2}{M_P} H_u H_d, \quad (56)$$

where H_u and H_d denote the up- and down-type Higgs doublets. In this case, $(H_u H_d)$ has a PQ charge of -2 and hence (some of) MSSM fields also have PQ charges. After ϕ obtains a VEV, equation 56 gives the higgsino mass, so-called μ -term, as $\mu = \lambda\eta^2/M_P$ and it is of the order of TeV for $\lambda = O(1)$ and $F_a \sim 10^{11}$ GeV. Thus the PQ scale may be related with the solution to the μ -problem in MSSM [97].

4.1.2 Model B

Let us consider the following superpotential,

$$W_{\text{PQ}} = \frac{\phi^n \bar{\phi}}{M^{n-2}}, \quad (57)$$

⁷ Recently it was proposed that the PQ scalars in superpotential 53 can take a role of waterfall field in hybrid inflation, while X is the inflaton [94, 95, 96]. A right amount of density perturbation is reproduced for $F_a \sim 10^{15}$ GeV.

⁸ To maintain the gauge coupling unification, it is often assumed that Q and \bar{Q} are complete multiplets of $\text{SU}(5)$ GUT gauge group.

where M denotes the cutoff scale and $n(\geq 3)$ is an integer. The PQ scalars ϕ and $\bar{\phi}$ have PQ charges of $+1$ and $-n$, respectively. The scalar potential after including the SUSY breaking effect is given by [98]

$$V = -m_s^2|\phi|^2 - m_{\bar{s}}^2|\bar{\phi}|^2 + \left(A_\phi \frac{\phi^n \bar{\phi}}{M^{n-2}} + \text{h.c.} \right) + \frac{|\phi|^{2(n-1)}}{M^{2(n-2)}} (|\phi|^2 + n^2|\bar{\phi}|^2), \quad (58)$$

where A_ϕ denotes the A -term contribution to the SUSY breaking potential. Here the soft mass squared of ϕ is assumed to have tachyonic form. Then ϕ is stabilized at

$$\eta = \langle \phi \rangle \sim (m_s M^{n-2})^{1/(n-1)}. \quad (59)$$

For example, for $n = 3$ and $M = M_P$, we have $\eta \sim \sqrt{m_s M_P}$ and it is of the order of 10^{11} GeV for the soft mass $m_s \sim 1$ TeV. The A -term also induces VEV of $\bar{\phi}$ as $\langle \bar{\phi} \rangle \sim A_\phi \eta / m_s$, which is smaller than η if $A_\phi < m_s$. The axino consists of mixtures of $\tilde{\phi}$ and $\tilde{\bar{\phi}}$, whose mass is given by $m_{\tilde{a}} \sim m_s$, as seen by substituting VEVs of ϕ and $\bar{\phi}$ into Equation 57. Note that the axino can be much heavier than the gravitino if $m_s \gg m_{3/2}$ due to gauge-mediation effect (see below).

4.1.3 Model C

In the above two models, we introduced two (or possibly more) PQ scalar fields for giving rise to the scalar potential. PQ scalars are stabilized by the combination of SUSY potential and SUSY breaking potential. However, there may be multiple sources of SUSY breaking effects. In the gauge-mediated SUSY breaking (GMSB) model, the dominant contribution to the soft SUSY breaking mass often comes from the GMSB effect, while small but non-negligible gravity-mediation effect generally exists. In particular, for a gauge-singlet scalar such as the PQ scalar, the effect of GMSB on its potential is rather non-trivial because it arises at higher loop level [99, 100, 101].

Let us consider the KSVZ model and see how the scalar potential is generated through the SUSY breaking effect. For simplicity, we adopt the following messenger sector

$$W_{\text{mess}} = \kappa X \Psi \bar{\Psi}, \quad (60)$$

where X denote the SUSY breaking field and Ψ and $\bar{\Psi}$ are messengers fields. For $k|\phi| \ll M_{\text{mess}}$, where M_{mess} is the messenger scale, the mass splitting on the scalar and fermionic

components of Q, \bar{Q} yield correction to the saxion mass. In the opposite case $k|\phi| \gg M_{\text{mess}}$, after integrating out the PQ quarks, the Kähler potential of the X field below the PQ scale is given by

$$\mathcal{L} = \int d^4\theta Z_X(|\phi|)|X|^2, \quad (61)$$

where the wave-function renormalization factor Z_X logarithmically depends on $|\phi|$ at the three-loop level. Thus we can estimate the PQ scalar potential as

$$|\phi| \frac{\partial V^{(\text{GM})}}{\partial |\phi|} \simeq \begin{cases} -\frac{4k^2}{\pi^2} m_s^2 |\phi|^2 & \text{for } k|\phi| \ll M_{\text{mess}} \\ -\frac{g_s^4 \kappa^2}{(4\pi^2)^3} |F_X|^2 \log^2\left(\frac{k|\phi|}{M_{\text{mess}}}\right) & \text{for } k|\phi| \gg M_{\text{mess}}. \end{cases} \quad (62)$$

where $m_s \equiv (g_s^2/16\pi^2)|F_X/X|$ is the typical soft mass induced by the GMSB effect. This potential has a negative slope, and hence PQ scalar is driven away from the origin. It can be stopped by other contributions. Since ϕ also feels the gravity-mediated SUSY breaking effect, there arises term

$$V^{(\text{grav})} \simeq m_{3/2}^2 |\phi|^2. \quad (63)$$

The PQ scalar can be stabilized by the balance between Equations 62 and 63 [100] as

$$\eta = \langle |\phi| \rangle \simeq \frac{g_s^2 \kappa |F_X|}{8\pi^3 m_{3/2}}, \quad (64)$$

if $k\eta > M_{\text{mess}}$. If X dominantly breaks SUSY, i.e., $|F_X| = \sqrt{3}m_{3/2}M_P$, we need small κ in order to obtain intermediated PQ scale. In this model, the axino is expected to obtain mass dominantly through radiative effect, which is evaluated as $m_{\tilde{a}} \simeq (k^2/16\pi^2)A_Q$, where A_Q denotes the A -term contribution to the KSVZ coupling : $\mathcal{L} = A_Q k \phi \tilde{Q} \tilde{\bar{Q}} + \text{h.c.}$ with $\tilde{Q}(\tilde{\bar{Q}})$ denoting the scalar component.

One can construct a variant of above mentioned models. For example, one can make use of the scalar potential induced by the term 57 to stabilize the PQ scalar against the potential 62 [102, 103, 104]. See also [105, 106, 107] for ideas to radiatively stabilize the PQ scalar.

4.2 Axino cosmology

The axinos are produced in the early Universe and they might cause cosmological disasters since the axino has a long lifetime. In the KSVZ model, the dominant axino production

process is scattering between gluons and gluinos through the axino-gluino-gluon interaction. The axino abundance, in terms of its number-to-entropy ratio, was evaluated as [108, 109, 110]

$$Y_a^{(g)} \equiv \frac{n_a^{(g)}}{s} \simeq 2 \times 10^{-6} g_s^6 \left(\frac{F_a}{10^{11} \text{ GeV}} \right)^{-2} \left(\frac{T_R}{10^5 \text{ GeV}} \right). \quad (65)$$

where T_R denotes the reheating temperature after inflation. In the DFSZ model, there is an axino-Higgs-higgsino interaction. Since this is Yukawa coupling with a coupling constant of $\sim \mu/F_a$, the axino production rate through the Higgs and higgsino scatterings increases at low temperature ($T \sim \mu$). The axino abundance in the DFSZ model in such a process is evaluated recently as [111, 112, 113]

$$Y_a^{(h)} \simeq 10^{-5} \left(\frac{F_a}{10^{11} \text{ GeV}} \right)^{-2} \left(\frac{\mu}{1 \text{ TeV}} \right)^2. \quad (66)$$

This contribution does not depend on the reheating temperature T_R .

Cosmological implication of the axino depends on whether it is the lightest SUSY particle (LSP) or not.⁹ If it is not the LSP, the axino decays into the neutralino whose abundance is limited from the observed DM abundance. If the neutralino annihilation cross section is fairly large, as in the case of higgsino or wino like neutralino, the axino decay can produce a right amount of neutralino for appropriate decay temperature of the axino [119, 120].

If the axino is the LSP, on the other hand, it can also be produced by the late decay of heavier SUSY particles. Actually, as shown previously, the axino mass is comparable to the gravitino mass, or it can be much lighter. In this case the axino abundance depends on the sparticle abundance after their freeze out. Thus if the sparticle annihilation cross section is not so small (i.e., if it would reproduce the DM abundance if it were the LSP), no significant constraint is imposed. Axinos are also produced by the gravitinos, which decay into axinos and axions [121]. In this case the resulting axino abundance depends on the gravitino abundance, which may be produced thermally or non-thermally (e.g., by the decay of inflaton). If the axino is much lighter than the gravitino, the constraint on the reheating temperature can be relaxed.

⁹ Evaluation of the axino mass is rather a delicate issue [114, 115, 116]. See also [117, 118] for recent calculations.

4.3 Saxion cosmology

Next let us consider the cosmological effects of the saxion. Saxions are produced thermally in a similar way to the axino, but there also exists a contribution from the coherent oscillation. The evaluation of the latter contribution is quite model dependent. As shown in previous section, there are many models of saxion stabilization, and the scalar field dynamics should be calculated in each PQ stabilization model. We here give a typical behavior of the saxion dynamics, but one should keep in mind that the dynamics can be far more complicated in some concrete models, which would result in orders of magnitude difference in the estimate of saxion abundance.

First, in the KSVZ model, the abundance of thermally produced saxions through the scattering by the gluons is given by [122]

$$Y_{\sigma}^{(g)} \equiv \frac{n_{\sigma}^{(g)}}{s} \simeq 2 \times 10^{-6} g_s^6 \left(\frac{F_a}{10^{11} \text{ GeV}} \right)^{-2} \left(\frac{T_R}{10^5 \text{ GeV}} \right). \quad (67)$$

As far as we have recognized, no detailed calculations were performed for the saxion abundance created by the saxion-higgsino or saxion-Higgs interactions in the DFSZ model (denoted by $Y_{\sigma}^{(h)}$ hereafter), but we reasonably expect that it is same order as the corresponding axino abundance (Equation 66).

As for the coherent oscillation, we first focus on the Model A in Sec. 4.1. In this case, the saxion feels the Hubble-induced mass in the early Universe and hence the saxion sits at the minimum determined by the Hubble mass if the Hubble-induced mass squared has positive coefficients. At $H \sim m_s$, the saxion begins to oscillate around the true minimum with initial amplitude σ_i . The abundance is thus given by

$$\frac{\rho_{\sigma}^{(\text{CO})}}{s} = \begin{cases} \frac{1}{8} T_R \left(\frac{\sigma_i}{M_P} \right)^2 \simeq 2 \times 10^{-11} \text{ GeV} \left(\frac{T_R}{10^5 \text{ GeV}} \right) \left(\frac{F_a}{10^{11} \text{ GeV}} \right)^2 \left(\frac{\sigma_i}{F_a} \right)^2 & \text{for } T_R \lesssim T_{\text{os}} \\ \frac{1}{8} T_{\text{os}} \left(\frac{\sigma_i}{M_P} \right)^2 \simeq 2 \times 10^{-7} \text{ GeV} \left(\frac{m_{\sigma}}{1 \text{ GeV}} \right)^{1/2} \left(\frac{F_a}{10^{11} \text{ GeV}} \right)^2 \left(\frac{\sigma_i}{F_a} \right)^2 & \text{for } T_R \gtrsim T_{\text{os}} \end{cases} \quad (68)$$

where $T_{\text{os}} \equiv (10/\pi^2 g_*)^{1/4} \sqrt{m_{\sigma} M_P}$. Note that it does not take into account various effects which would modify the abundance significantly. For example, thermal effects modify the ϕ potential in the KSVZ model, which can change the saxion dynamics significantly [94, 95, 123]. Thermal corrections to the scalar potential are negligible in the DFSZ model. On the other hand, if the Hubble-mass squared has negative coefficient, the saxion is

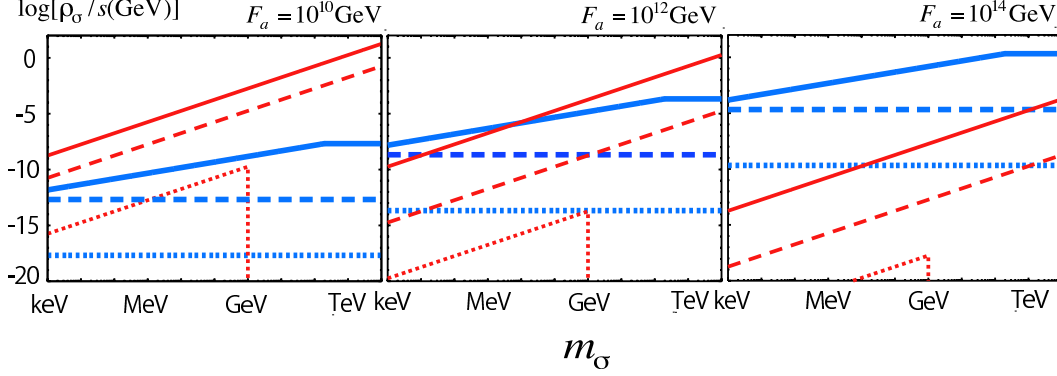


Figure 9: The saxion abundance as a function of saxion mass m_σ for $F_a = 10^{10}, 10^{12}, 10^{14}$ GeV from left to right. Thick blue lines correspond to $(\rho_\sigma/s)^{(\text{CO})}$ with $\sigma_i = F_a$ and thin red lines to $m_\sigma Y_\sigma^{(g)}$ in the KSVZ model. Solid, dashed and dotted lines correspond to $T_R = 10^{10}, 10^5$ and 1 GeV respectively.

driven away to $\sim M_P$ during inflation, hence we expect $\sigma_i \sim M_P$ in this case.¹⁰

The saxion abundance is given by sum of thermal contribution and coherent oscillation : $\rho_\sigma/s = (\rho_\sigma/s)^{(\text{CO})} + m_\sigma (Y_\sigma^{(g)} + Y_\sigma^{(h)})$. Figure 9 shows it for the KSVZ model. The saxion abundance is bounded above from cosmological/astrophysical arguments depending on the saxion lifetime. Here we list relevant constraints depending on the saxion lifetime τ_σ [126].

- $\tau_\sigma \lesssim 10^{12}$ sec : The axion produced by the saxion decay should not contribute to the effective number of neutrino species too much. Conversely, it can explain the recent observational claim of the existence of dark radiation [127, 95, 128, 129, 130].
- $1 \text{ sec} \lesssim \tau_\sigma \lesssim 10^{12} \text{ sec}$: Injected visible energy by the saxion decay should not alter the abundance of light elements synthesized by the big-bang nucleosynthesis (BBN).
- $10^6 \text{ sec} \lesssim \tau_\sigma \lesssim 10^{12} \text{ sec}$: Injected visible energy by the saxion decay should not distort the blackbody spectrum of CMB.
- $\tau_\sigma \gtrsim 10^{12} \text{ sec}$: Photons produced by the saxion decay should not exceed the observed diffuse extragalactic background photon spectrum.

¹⁰ In such a case ($\sigma_i \sim M_P$), the axion isocurvature perturbation is suppressed, because it is proportional to $\delta\theta/\theta = \delta\theta_i/\theta_i \sim H_{\text{inf}}/\sigma_i$ [124]. On the other hand, if the coefficients are mildly positive, it is possible to create the axion isocurvature perturbation with extremely blue spectrum by considering the dynamics of saxion during inflation [125].

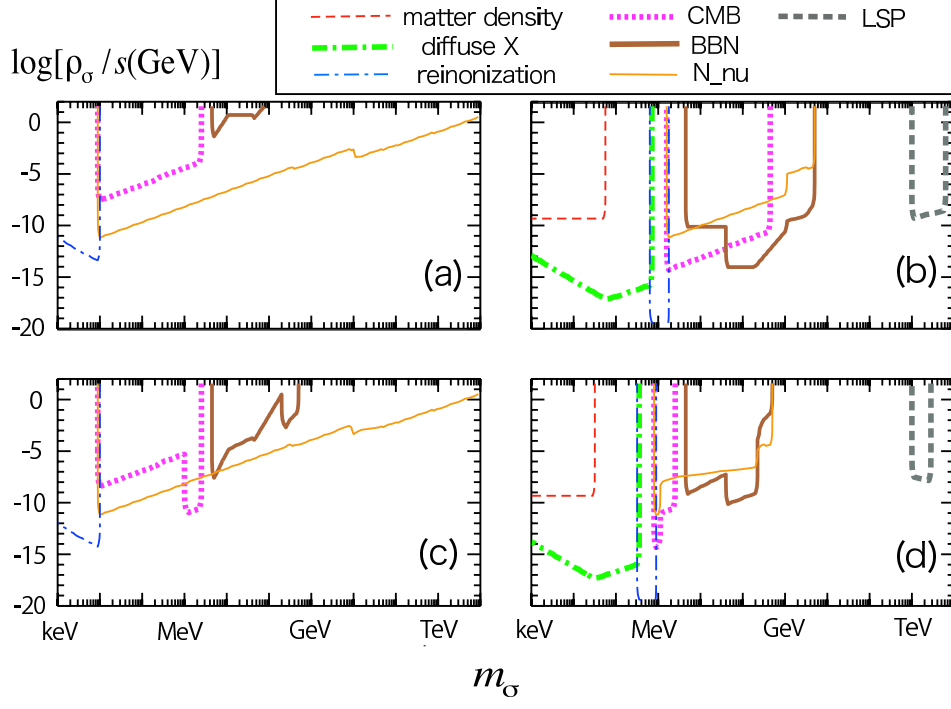


Figure 10: Cosmological constraints on the saxion abundance as a function of saxion mass m_σ for $F_a = 10^{10}$ GeV in the KSVZ model ((a) and (b)) and DFSZ model ((c) and (d)). In (a) and (c), the saxion decay into axions is assumed to be unsuppressed. In (b) and (d), it is assumed to be suppressed. See [126] for more detail.

- $\tau_\sigma \gtrsim 10^{12}$ sec : Injected photons should not ionize the neutral hydrogen too much, which would otherwise leads to too early epoch of reionization.
- $\tau_\sigma \gtrsim 10^{17}$ sec : The saxion abundance itself should not exceed the observed DM abundance.

These set bound on the saxion abundance and reheating temperature for every mass range of the saxion. Figure 10 shows cosmological constraints on the saxion abundance for a wide range of the saxion mass. For more details on these constraints, see [126] and references therein.

For Models B and C, the saxion is likely trapped at the origin $\phi = 0$ due to thermal effects in KSVZ-type models. In this case, thermal inflation [131] takes place because of the potential energy $V(|\phi| = 0)$. After thermal inflation, the saxion oscillation dominates the Universe and its decay causes the reheating. Cosmological implications of such a

scenario were discussed in [132, 133, 134, 135, 136, 137]. It should be noticed that the domain wall number N_{DW} must be equal to one in order to avoid the axionic domain wall problem (see Section 3.3).

5 Discussion

We have reviewed recent developments in the field of axion cosmology and its SUSY version. In particular, according to recent simulations on axion emissions from axionic strings and domain walls, the upper bound on the PQ scale reads $F_a \lesssim (2.0 - 3.8) \times 10^{10} \text{ GeV}$ for $N_{\text{DW}} = 1$ if the PQ symmetry is broken after inflation. There is no room for the case of $N_{\text{DW}} \geq 2$ unless the phase of explicit PQ breaking bias term is finely tuned. This gives a tight bound on the PQ model. If the PQ symmetry is broken before/during inflation, this constraint does not apply. Instead, the constraint from axion isocurvature perturbations requires low inflation energy scale. Recent investigations on non-Gaussianity in the isocurvature perturbation has shown that it gives comparable constraint to that from the analysis of CMB power spectrum. We have also reviewed SUSY axion models with some explicit examples of saxion stabilization. Recent studies on cosmology of saxion and axino are briefly discussed.

Below we list some recent topics related to the axion physics which were not covered in the main text.

Axion thermalization In a recent series of works [138, 139, 140] it was pointed out that the cold axion thermalizes by the gravitational interaction and forms Bose-Einstein condensate, which also leads to drastic effects on the effective number of neutrinos through the effective photon-axion interaction. Currently there are little discussions on this claim and more investigations will be necessary (see also [141]).

SUSY axion model with 125 GeV Higgs After the discovery of the 125 GeV Higgs-like scalar boson [1, 2], many models were proposed in SUSY framework. Some of them are closely related to the axion solution to the strong CP problem. In [104], vector-like matter was introduced for raising the lightest Higgs mass while the PQ symmetry plays

an essential role to explain the appropriate mass of the vector-like matter and to solve the μ -problem. In [142, 143], a singlet extension of the MSSM was considered for raising the lightest Higgs mass, where an appropriate value for the tadpole term in the singlet sector is explained by the PQ symmetry. Further LHC data may be able to confirm such a scenario.

String axion and axiverse Finally, we want to make a brief comment on realization of the QCD axion in the string theory. The origin of global PQ symmetry is somewhat mysterious since even the Planck-suppressed PQ violating operators must be highly controlled. In string theory, such a shift symmetry of the axion-like field often appears after the compactification of extra dimensions in the zero-modes of the dilaton, NS-NS 2-form and R-R p -forms with $p = 1, 3$ in type IIA and $p = 0, 2, 4$ in type IIB theories (see e.g. [144]). These fields acquire masses from non-perturbative effects which break the shift symmetry. Since these effects exponentially depend on various parameters, axions with wide mass ranges in logarithmic scale are expected to exist, one of which may be the QCD axion: the so-called string axiverse scenario [145]. Here one should ensure that the mechanism of saxion/moduli stabilization does not give rise to the axion mass. This severely restricts the stabilization mechanism, and discussions on this topic are found in [146, 147, 148, 149, 150] mostly for the type IIB theory. Once a successful saxion stabilization mechanism is identified, its cosmological effects can be discussed. It will be an interesting topic which has not been investigated in detail so far.

Acknowledgment

This work is supported by Grant-in-Aid for Scientific research from the Ministry of Education, Science, Sports, and Culture (MEXT), Japan, No. 14102004 (M.K.), No. 21111006 (M.K. and K.N.), No. 22244030 (K.N.) and also by World Premier International Research Center Initiative (WPI Initiative), MEXT, Japan.

References

- [1] G. Aad *et al.* [ATLAS Collaboration], Phys. Lett. B **716**, 1 (2012) [arXiv:1207.7214 [hep-ex]].
- [2] S. Chatrchyan *et al.* [CMS Collaboration], Phys. Lett. B **716**, 30 (2012) [arXiv:1207.7235 [hep-ex]].
- [3] J. E. Kim, Phys. Rept. **150**, 1 (1987).
- [4] J. E. Kim and G. Carosi, Rev. Mod. Phys. **82**, 557 (2010) [arXiv:0807.3125 [hep-ph]].
- [5] C. A. Baker *et al.*, Phys. Rev. Lett. **97**, 131801 (2006) [arXiv:hep-ex/0602020].
- [6] R. D. Peccei and H. R. Quinn, Phys. Rev. Lett. **38**, 1440 (1977).
- [7] R. D. Peccei and H. R. Quinn, Phys. Rev. D **16**, 1791 (1977).
- [8] S. Weinberg, Phys. Rev. Lett. **40**, 223 (1978).
- [9] F. Wilczek, Phys. Rev. Lett. **40**, 279 (1978).
- [10] J. E. Kim, Phys. Rev. Lett. **43**, 103 (1979).
- [11] M. A. Shifman, A. I. Vainshtein, V. I. Zakharov, Nucl. Phys. **B166**, 493 (1980).
- [12] M. Dine, W. Fischler and M. Srednicki, Phys. Lett. B **104**, 199 (1981);
- [13] A. R. Zhitnitsky, Sov. J. Nucl. Phys. **31**, 260 (1980) [Yad. Fiz. **31**, 497 (1980)].
- [14] R. D. Peccei, T. T. Wu and T. Yanagida, Phys. Lett. B **172**, 435 (1986).
- [15] L. M. Krauss and F. Wilczek, Phys. Lett. B **173**, 189 (1986).
- [16] C. -R. Chen, P. H. Frampton, F. Takahashi and T. T. Yanagida, JHEP **1006**, 059 (2010) [arXiv:1005.1185 [hep-ph]].
- [17] G. G. Raffelt, “Stars as laboratories for fundamental physics: The astrophysics of neutrinos, axions, and other weakly interacting particles,” Chicago, USA: Univ. Pr. (1996).
- [18] G. G. Raffelt, Ann. Rev. Nucl. Part. Sci. **49**, 163 (1999) [hep-ph/9903472].
- [19] S. Chang and K. Choi, Phys. Lett. B **316**, 51 (1993) [hep-ph/9306216].
- [20] T. Moroi and H. Murayama, Phys. Lett. B **440**, 69 (1998) [hep-ph/9804291].

- [21] P. Sikivie, Phys. Rev. Lett. **51**, 1415 (1983) [Erratum-ibid. **52**, 695 (1984)].
- [22] E. Arik *et al.* [CAST Collaboration], JCAP **0902**, 008 (2009) [arXiv:0810.4482 [hep-ex]].
- [23] S. Aune *et al.* [CAST Collaboration], Phys. Rev. Lett. **107**, 261302 (2011) [arXiv:1106.3919 [hep-ex]].
- [24] Y. Inoue, Y. Akimoto, R. Ohta, T. Mizumoto, A. Yamamoto and M. Minowa, Phys. Lett. B **668**, 93 (2008) [arXiv:0806.2230 [astro-ph]].
- [25] I. G. Irastorza *et al.*, JCAP **1106**, 013 (2011) [arXiv:1103.5334 [hep-ex]].
- [26] R. Bradley, J. Clarke, D. Kinion, L. J. Rosenberg, K. van Bibber, S. Matsuki, M. Muck and P. Sikivie, Rev. Mod. Phys. **75**, 777 (2003).
- [27] S. J. Asztalos *et al.* [The ADMX Collaboration], Phys. Rev. Lett. **104**, 041301 (2010) [arXiv:0910.5914 [astro-ph.CO]].
- [28] K. Ehret, M. Frede, S. Ghazaryan, M. Hildebrandt, E. -A. Knabbe, D. Kracht, A. Lindner and J. List *et al.*, Phys. Lett. B **689**, 149 (2010) [arXiv:1004.1313 [hep-ex]].
- [29] P. Sikivie, D. B. Tanner and K. van Bibber, Phys. Rev. Lett. **98**, 172002 (2007) [hep-ph/0701198 [HEP-PH]].
- [30] J. E. Moody and F. Wilczek, Phys. Rev. D **30**, 130 (1984).
- [31] B. R. Heckel, C. E. Cramer, T. S. Cook, E. G. Adelberger, S. Schlamminger and U. Schmidt, Phys. Rev. Lett. **97**, 021603 (2006) [hep-ph/0606218].
- [32] S. A. Hoedl, F. Fleischer, E. G. Adelberger and B. R. Heckel, Phys. Rev. Lett. **106**, 041801 (2011).
- [33] G. Raffelt, Phys. Rev. D **86**, 015001 (2012) [arXiv:1205.1776 [hep-ph]].
- [34] P. W. Graham and S. Rajendran, Phys. Rev. D **84**, 055013 (2011) [arXiv:1101.2691 [hep-ph]].
- [35] K. J. Bae, J. -H. Huh and J. E. Kim, JCAP **0809**, 005 (2008) [arXiv:0806.0497 [hep-ph]].
- [36] D. J. Gross, R. D. Pisarski and L. G. Yaffe, Rev. Mod. Phys. **53**, 43 (1981).

- [37] O. Wantz and E. P. S. Shellard, Phys. Rev. D **82**, 123508 (2010) [arXiv:0910.1066 [astro-ph.CO]].
- [38] O. Wantz and E. P. S. Shellard, Nucl. Phys. B **829**, 110 (2010) [arXiv:0908.0324 [hep-ph]].
- [39] K. J. Bae, J. -H. Huh and J. E. Kim, JCAP **0809**, 005 (2008) [arXiv:0806.0497 [hep-ph]].
- [40] M. S. Turner, Phys. Rev. D **33**, 889 (1986).
- [41] D. H. Lyth, Phys. Rev. D **45**, 3394 (1992).
- [42] M. Kawasaki, T. Moroi and T. Yanagida, Phys. Lett. B **383**, 313 (1996) [hep-ph/9510461].
- [43] E. Masso, F. Rota and G. Zsembinski, Phys. Rev. D **66**, 023004 (2002) [hep-ph/0203221].
- [44] P. Graf and F. D. Steffen, Phys. Rev. D **83**, 075011 (2011) [arXiv:1008.4528 [hep-ph]].
- [45] S. Hannestad, A. Mirizzi and G. Raffelt, JCAP **0507**, 002 (2005) [hep-ph/0504059].
- [46] S. Hannestad, A. Mirizzi, G. G. Raffelt and Y. Y. Y. Wong, JCAP **1008**, 001 (2010) [arXiv:1004.0695 [astro-ph.CO]].
- [47] M. Yamaguchi, J. 'i. Yokoyama and M. Kawasaki, Prog. Theor. Phys. **100**, 535 (1998) [hep-ph/9808326].
- [48] M. Yamaguchi, M. Kawasaki and J. 'i. Yokoyama, Phys. Rev. Lett. **82**, 4578 (1999) [hep-ph/9811311].
- [49] M. Yamaguchi, J. 'i. Yokoyama and M. Kawasaki, Phys. Rev. D **61**, 061301 (2000) [hep-ph/9910352].
- [50] T. Hiramatsu, M. Kawasaki, T. Sekiguchi, M. Yamaguchi and J. 'i. Yokoyama, Phys. Rev. D **83**, 123531 (2011) [arXiv:1012.5502 [hep-ph]].
- [51] R. L. Davis, Phys. Lett. B **180**, 225 (1986).
- [52] R. L. Davis and E. P. S. Shellard, Nucl. Phys. B **324**, 167 (1989).
- [53] A. Dabholkar and J. M. Quashnock, Nucl. Phys. B **333**, 815 (1990).

- [54] D. Harari and P. Sikivie, Phys. Lett. B **195**, 361 (1987).
- [55] C. Hagmann and P. Sikivie, Nucl. Phys. B **363**, 247 (1991).
- [56] C. Hagmann, S. Chang and P. Sikivie, Phys. Rev. D **63**, 125018 (2001) [hep-ph/0012361].
- [57] T. Hiramatsu, M. Kawasaki and K. i. Saikawa, JCAP **1108**, 030 (2011) [arXiv:1012.4558 [astro-ph.CO]].
- [58] T. Hiramatsu, M. Kawasaki, K. i. Saikawa and T. Sekiguchi, Phys. Rev. D **85**, 105020 (2012) [Erratum-ibid. D **86**, 089902 (2012)] [arXiv:1202.5851 [hep-ph]].
- [59] M. Nagasawa and M. Kawasaki, Phys. Rev. D **50**, 4821 (1994) [astro-ph/9402066].
- [60] S. Chang, C. Hagmann and P. Sikivie, Phys. Rev. D **59**, 023505 (1999) [hep-ph/9807374].
- [61] C. Hagmann, S. Chang and P. Sikivie, Nucl. Phys. Proc. Suppl. **72**, 81 (1999) [hep-ph/9807428].
- [62] B. S. Ryden, W. H. Press and D. N. Spergel, Astrophys. J. **357**, 293 (1990).
- [63] T. Hiramatsu, M. Kawasaki, K. i. Saikawa and T. Sekiguchi, arXiv:1207.3166 [hep-ph].
- [64] M. Axenides, R. H. Brandenberger, M. S. Turner, Phys. Lett. B **126**, 178 (1983).
- [65] D. Seckel, M. S. Turner, Phys. Rev. D **32**, 3178 (1985).
- [66] A. D. Linde, Phys. Lett. B **158**, 375-380 (1985).
- [67] A. D. Linde, D. H. Lyth, Phys. Lett. B **246**, 353-358 (1990).
- [68] M. S. Turner, F. Wilczek, Phys. Rev. Lett. **66**, 5 (1991).
- [69] A. D. Linde, Phys. Lett. B **259**, 38 (1991).
- [70] M. Sasaki and E. D. Stewart, Prog. Theor. Phys. **95**, 71 (1996) [astro-ph/9507001].
- [71] D. H. Lyth, K. A. Malik and M. Sasaki, JCAP **0505**, 004 (2005) [astro-ph/0411220].
- [72] K. Moodley, M. Bucher, J. Dunkley, P. G. Ferreira and C. Skordis, Phys. Rev. D **70**, 103520 (2004) [astro-ph/0407304].

- [73] M. Beltran, J. Garcia-Bellido, J. Lesgourgues and A. Riazuelo, Phys. Rev. D **70**, 103530 (2004) [astro-ph/0409326].
- [74] R. Bean, J. Dunkley and E. Pierpaoli, Phys. Rev. D **74**, 063503 (2006) [astro-ph/0606685].
- [75] R. Trotta, Mon. Not. Roy. Astron. Soc. **375**, L26 (2007) [astro-ph/0608116].
- [76] R. Keskitalo, H. Kurki-Suonio, V. Muhonen and J. Valiviita, JCAP **0709**, 008 (2007) [astro-ph/0611917].
- [77] M. Kawasaki and T. Sekiguchi, Prog. Theor. Phys. **120**, 995 (2008) [arXiv:0705.2853 [astro-ph]].
- [78] I. Sollom, A. Challinor and M. P. Hobson, Phys. Rev. D **79**, 123521 (2009) [arXiv:0903.5257 [astro-ph.CO]].
- [79] J. Valiviita, M. Savelainen, M. Talvitie, H. Kurki-Suonio and S. Rusak, Astrophys. J. **753**, 151 (2012) [arXiv:1202.2852 [astro-ph.CO]].
- [80] E. Komatsu *et al.* [WMAP Collaboration], Astrophys. J. Suppl. **192**, 18 (2011) [arXiv:1001.4538 [astro-ph.CO]].
- [81] L. Boubekur and D. H. Lyth, Phys. Rev. D **73**, 021301 (2006) [astro-ph/0504046].
- [82] M. Kawasaki, K. Nakayama, T. Sekiguchi, T. Suyama and F. Takahashi, JCAP **0811**, 019 (2008) [arXiv:0808.0009 [astro-ph]].
- [83] D. Langlois, F. Vernizzi and D. Wands, JCAP **0812**, 004 (2008) [arXiv:0809.4646 [astro-ph]].
- [84] M. Kawasaki, K. Nakayama, T. Sekiguchi, T. Suyama and F. Takahashi, JCAP **0901**, 042 (2009) [arXiv:0810.0208 [astro-ph]].
- [85] E. Kawakami, M. Kawasaki, K. Nakayama and F. Takahashi, JCAP **0909**, 002 (2009) [arXiv:0905.1552 [astro-ph.CO]].
- [86] D. Langlois and A. Lepidi, JCAP **1101**, 008 (2011) [arXiv:1007.5498 [astro-ph.CO]].
- [87] D. Langlois and T. Takahashi, JCAP **1102**, 020 (2011) [arXiv:1012.4885 [astro-ph.CO]].

- [88] D. Langlois and B. van Tent, JCAP **1207**, 040 (2012) [arXiv:1204.5042 [astro-ph.CO]].
- [89] C. Hikage, K. Koyama, T. Matsubara, T. Takahashi and M. Yamaguchi, Mon. Not. Roy. Astron. Soc. **398**, 2188 (2009) [arXiv:0812.3500 [astro-ph]].
- [90] C. Hikage, M. Kawasaki, T. Sekiguchi and T. Takahashi, arXiv:1211.1095 [astro-ph.CO].
- [91] T. Kugo, I. Ojima and T. Yanagida, Phys. Lett. B **135**, 402 (1984).
- [92] K. Tamvakis and D. Wyler, Phys. Lett. B **112**, 451 (1982).
- [93] K. Rajagopal, M. S. Turner and F. Wilczek, Nucl. Phys. B **358**, 447 (1991).
- [94] M. Kawasaki, N. Kitajima and K. Nakayama, Phys. Rev. D **82**, 123531 (2010) [arXiv:1008.5013 [hep-ph]].
- [95] M. Kawasaki, N. Kitajima and K. Nakayama, Phys. Rev. D **83**, 123521 (2011) [arXiv:1104.1262 [hep-ph]].
- [96] M. Kawasaki, N. Kitajima and K. Nakayama, arXiv:1211.6516 [hep-ph].
- [97] J. E. Kim and H. P. Nilles, Phys. Lett. B **138**, 150 (1984).
- [98] H. Murayama, H. Suzuki and T. Yanagida, Phys. Lett. B **291**, 418 (1992).
- [99] N. Arkani-Hamed, G. F. Giudice, M. A. Luty and R. Rattazzi, Phys. Rev. D **58**, 115005 (1998) [hep-ph/9803290].
- [100] T. Asaka and M. Yamaguchi, Phys. Lett. B **437**, 51 (1998) [hep-ph/9805449].
- [101] T. Asaka and M. Yamaguchi, Phys. Rev. D **59**, 125003 (1999) [hep-ph/9811451].
- [102] T. Banks, M. Dine and M. Graesser, Phys. Rev. D **68**, 075011 (2003) [hep-ph/0210256].
- [103] K. Choi, E. J. Chun, H. D. Kim, W. I. Park and C. S. Shin, Phys. Rev. D **83**, 123503 (2011) [arXiv:1102.2900 [hep-ph]].
- [104] K. Nakayama and N. Yokozaki, JHEP **1211**, 158 (2012) [arXiv:1204.5420 [hep-ph]].
- [105] N. Abe, T. Moroi and M. Yamaguchi, JHEP **0201**, 010 (2002) [hep-ph/0111155].

- [106] S. Nakamura, K. -i. Okumura and M. Yamaguchi, Phys. Rev. D **77**, 115027 (2008) [arXiv:0803.3725 [hep-ph]].
- [107] K. S. Jeong and M. Yamaguchi, JHEP **1107**, 124 (2011) [arXiv:1102.3301 [hep-ph]].
- [108] L. Covi, H. -B. Kim, J. E. Kim and L. Roszkowski, JHEP **0105**, 033 (2001) [hep-ph/0101009].
- [109] A. Brandenburg and F. D. Steffen, JCAP **0408**, 008 (2004) [hep-ph/0405158].
- [110] A. Strumia, JHEP **1006**, 036 (2010) [arXiv:1003.5847 [hep-ph]].
- [111] E. J. Chun, Phys. Rev. D **84**, 043509 (2011) [arXiv:1104.2219 [hep-ph]].
- [112] K. J. Bae, K. Choi and S. H. Im, JHEP **1108**, 065 (2011) [arXiv:1106.2452 [hep-ph]].
- [113] K. J. Bae, E. J. Chun and S. H. Im, JCAP **1203**, 013 (2012) [arXiv:1111.5962 [hep-ph]].
- [114] T. Goto and M. Yamaguchi, Phys. Lett. B **276**, 103 (1992).
- [115] E. J. Chun, J. E. Kim and H. P. Nilles, Phys. Lett. B **287**, 123 (1992) [hep-ph/9205229].
- [116] E. J. Chun and A. Lukas, Phys. Lett. B **357**, 43 (1995) [hep-ph/9503233].
- [117] T. Higaki and R. Kitano, Phys. Rev. D **86**, 075027 (2012) [arXiv:1104.0170 [hep-ph]].
- [118] J. E. Kim and M. -S. Seo, Nucl. Phys. B **864**, 296 (2012) [arXiv:1204.5495 [hep-ph]].
- [119] K. -Y. Choi, J. E. Kim, H. M. Lee and O. Seto, Phys. Rev. D **77**, 123501 (2008) [arXiv:0801.0491 [hep-ph]].
- [120] H. Baer, A. Lessa and W. Sreethawong, JCAP **1201**, 036 (2012) [arXiv:1110.2491 [hep-ph]].
- [121] T. Asaka and T. Yanagida, Phys. Lett. B **494**, 297 (2000) [hep-ph/0006211].
- [122] P. Graf and F. D. Steffen, arXiv:1208.2951 [hep-ph].
- [123] T. Moroi and M. Takimoto, Phys. Lett. B **718**, 105 (2012) [arXiv:1207.4858 [hep-ph]].

- [124] M. Kawasaki and K. Nakayama, Phys. Rev. D **77**, 123524 (2008) [arXiv:0802.2487 [hep-ph]].
- [125] S. Kasuya and M. Kawasaki, Phys. Rev. D **80**, 023516 (2009) [arXiv:0904.3800 [astro-ph.CO]].
- [126] M. Kawasaki, K. Nakayama and M. Senami, JCAP **0803**, 009 (2008) [arXiv:0711.3083 [hep-ph]].
- [127] K. Ichikawa, M. Kawasaki, K. Nakayama, M. Senami and F. Takahashi, JCAP **0705**, 008 (2007) [hep-ph/0703034 [HEP-PH]].
- [128] M. Kawasaki, K. Miyamoto, K. Nakayama and T. Sekiguchi, JCAP **1202**, 022 (2012) [arXiv:1107.4962 [astro-ph.CO]].
- [129] K. S. Jeong and F. Takahashi, JHEP **1208**, 017 (2012) [arXiv:1201.4816 [hep-ph]].
- [130] K. Choi, K. -Y. Choi and C. S. Shin, Phys. Rev. D **86**, 083529 (2012) [arXiv:1208.2496 [hep-ph]].
- [131] D. H. Lyth and E. D. Stewart, Phys. Rev. D **53**, 1784 (1996) [hep-ph/9510204].
- [132] E. D. Stewart, M. Kawasaki and T. Yanagida, Phys. Rev. D **54**, 6032 (1996) [hep-ph/9603324].
- [133] K. Choi, E. J. Chun and J. E. Kim, Phys. Lett. B **403**, 209 (1997) [hep-ph/9608222].
- [134] E. J. Chun, D. Comelli and D. H. Lyth, Phys. Rev. D **62**, 095013 (2000) [hep-ph/0008133].
- [135] S. Kim, W. -I. Park and E. D. Stewart, JHEP **0901**, 015 (2009) [arXiv:0807.3607 [hep-ph]].
- [136] K. Choi, K. S. Jeong, W. -I. Park and C. S. Shin, JCAP **0911**, 018 (2009) [arXiv:0908.2154 [hep-ph]].
- [137] W. -I. Park, JHEP **1007**, 085 (2010) [arXiv:1004.2326 [hep-ph]].
- [138] P. Sikivie and Q. Yang, Phys. Rev. Lett. **103**, 111301 (2009) [arXiv:0901.1106 [hep-ph]].
- [139] O. Erken, P. Sikivie, H. Tam and Q. Yang, Phys. Rev. Lett. **108**, 061304 (2012) [arXiv:1104.4507 [astro-ph.CO]].

- [140] O. Erken, P. Sikivie, H. Tam and Q. Yang, Phys. Rev. D **85**, 063520 (2012) [arXiv:1111.1157 [astro-ph.CO]].
- [141] K. 'i. Saikawa and M. Yamaguchi, arXiv:1210.7080 [hep-ph].
- [142] K. S. Jeong, Y. Shoji and M. Yamaguchi, JHEP **1209**, 007 (2012) [arXiv:1205.2486 [hep-ph]].
- [143] K. J. Bae, K. Choi, E. J. Chun, S. H. Im, C. B. Park and C. S. Shin, arXiv:1208.2555 [hep-ph].
- [144] P. Svrcek and E. Witten, JHEP **0606**, 051 (2006) [hep-th/0605206].
- [145] A. Arvanitaki, S. Dimopoulos, S. Dubovsky, N. Kaloper and J. March-Russell, Phys. Rev. D **81**, 123530 (2010) [arXiv:0905.4720 [hep-th]].
- [146] J. P. Conlon, JHEP **0605**, 078 (2006) [hep-th/0602233].
- [147] K. Choi and K. S. Jeong, JHEP **0701**, 103 (2007) [hep-th/0611279].
- [148] M. Dine, G. Festuccia, J. Kehayias and W. Wu, JHEP **1101**, 012 (2011) [arXiv:1010.4803 [hep-th]].
- [149] T. Higaki and T. Kobayashi, Phys. Rev. D **84**, 045021 (2011) [arXiv:1106.1293 [hep-th]].
- [150] M. Cicoli, M. Goodsell, A. Ringwald, JHEP **1210**, 146 (2012) [arXiv:1206.0819 [hep-th]].